Available online at www.sciencedirect.com
SciVerse ScienceDirect
Journal of the European Ceramic Society xxx (2012) xxx–xxx
www.elsevier.com/locate/jeurceramsoc

Correlation between $MgAl_2O_4$-spinel structure, processing factors and functional properties of transparent parts (progress review)

Adrian Goldstein *

Israel Ceramic and Silicate Institute, Technion City, 32000 Haifa, Israel

Abstract

Efforts were and are made to develop performant fabrication technologies, for transparent polycrystalline spinel – a material used for armor, infrared windows and other products. Significant progress was made – during some fifty years of research – regarding the understanding of the structure of spinel, at various scales, and the best ways to correlate processing with the relevant structural features so as to improve properties. This review compiles and comments the results of this progress, using as sources the literature and the author's own work. As of now the best specimens obtained combine submicron grains with an optical transmission close to the theoretical and a Vickers hardness of 15 GPa (size ≤25 cm). Larger plates, more than 0.5 m in size, but with coarse microstructure and lower hardness, have also been produced, together with quite large dome shaped parts, exhibiting highly uniform optical properties.
© 2012 Elsevier Ltd. All rights reserved.

Keywords: Sintering; Grain size; Defects; Optical properties; Spinel

1. Introduction

1.1. Applications of transparent spinel

Polycrystalline $MgAl_2O_4$-spinel (Sp) may exhibit, when properly processed, a combination of properties including optical transparency (it is a cubic, isotropic crystal), making it useful – together with other transparent ceramics like polycrystalline AlON or α-Al_2O_3 (single or polycrystal) – for the obtainment of armor window strike-faces and protective windows for sensors operating in the mid infrared (MIR) range.[1–6] It was measured, for instance, that panels of spinel needed to stop a given type of projectile had an areal density 60% lower than that of panels made exclusively of glass, outperforming also single-crystal sapphire.[7] These applications are the main reason for the great interest existent, for a long time now, in the development of technologies allowing the fabrication of transparent polycrystalline spinel parts.

Transparent spinel is a useful material also for other interesting products, including windows for barcode reader, pressure vessel or laser spark plug, tunable laser (Ti) hosts, high index optics for ultraviolet (UV) microlithography, high pressure arc lamps, watch casings, optical heat exchangers, etc.[6,8,10]

1.2. Main objectives of current engineering research

Moderately transparent spinel was demonstrated already in the late sixties by US researchers, and by the end of the eighties high transmission parts were obtained,[1–5] in small numbers, in the US, Japan and France; most of the early progress was owed to a few teams led or including D.W. Roy.[2,5] Nonetheless research and development efforts continue to this day. One of the main goals of this effort is the perfecting of satisfactory spinel fabrication technologies. A satisfactory technology means one able to generate commercially viable transparent[11] spinel parts, i.e. ones which simultaneously exhibit good performance, the desired size and shape, and are available in sufficient amounts at a reasonable price. While obtainment of transparent spinel which exhibits only one or two of the needed features is a task of moderate difficulty, establishment of technologies responding to all the requirements is a much more challenging goal, not fully achieved yet, despite some fifty years of effort.

A second research topic, which received an increased attention lately, is the development of transparent spinel exhibiting

* Tel.: +972 4 8222107/8; fax: +972 4 8325339.
E-mail address: goldaad@actcom.net.il

0955-2219/$ – see front matter © 2012 Elsevier Ltd. All rights reserved.
doi:10.1016/j.jeurceramsoc.2012.02.051

Please cite this article in press as: Goldstein A. Correlation between $MgAl_2O_4$-spinel structure, processing factors and functional properties of transparent parts (progress review). *J. Eur. Ceram. Soc.* (2012), doi:10.1016/j.jeurceramsoc.2012.02.051

an optimal balance between the transmittance and the functional properties (the mechanical characteristics being the most important). In fact, obtainment of fine grained (essential feature for good mechanical properties) transparent spinel was tried early.[12] Specimens exhibiting an average grains size ($\overline{GS}$) of just 1 μm have been obtained, using a special incremental hot pressing schedule, but the level of transparency attained was modest. In the following decades sintering at high temperatures was used by most research teams, especially in the US, in order to improve optical transmission. The large grains size (50–300 μm) thus generated had a deleterious effect on mechanical properties; hardness values reported were limited to around 12 GPa.[13–15] More recent research, in which new, better processing approaches were developed, succeeded in dramatically reducing the grain size while keeping transmittance close to the theoretical level; as a result hardness was raised toward the 15 GPa level.[16] Further improvements of the balance between transparency and mechanical properties are one of the main goals of current efforts.

1.3. Structural features which influence transparent spinel performance: requirements

As noted above, in the case of transparent spinel, high performance requires, in most cases, a combination of high in-line optical transmission (ILT) with good mechanical properties.[2,5,6,9] Various features of the structure, at the atomic or nano/micro scales, determine the performance controlling properties. The most important such features are discussed in this section.

For good mechanical properties (including suitable behavior after impact by high velocity projectiles and resistance to erosion) it is important to keep the $\overline{GS}$ as low (<5 μm, with submicron being best)[1,2,5,6,8,10,16] as possible. In order to fully exploit the benefits of a low $\overline{GS}$ the amount of macroscopic processing defects – such as cracks, pits, delamination voids, residual stress and porosity – has to be severely limited (excessive amounts of dislocations are also deleterious). The theoretical limits for these properties are not known. The values achieved in practice will be discussed in Section 3 and Tables 1 and 2.

Table 1
Range of values of transparent spinel performance-controlling properties reported by the literature.

Characteristics		Range of values
ILT	[%]	75–85 (λ = 750 nm; for t = 3–1 mm in most cases)
$\overline{GS}$	[μm]	0.4–120
HV	[GPa]	12.0–15.0 (for testing loads 5 and 10 kg)
TRS	[MPa]	150–250
E	[GPa]	260–310
$\alpha_{85-1000\,^\circ C}$	[$^\circ C^{-1}$]	77–80
λ_{th}	[W m^{-1} $^\circ$K^{-1}]	10–15

For high ILT Eq. (1) – which describes the dependence of ILT on the characteristics of the electromagnetic radiation – suggests the relevant factors of influence.

$$\mathrm{ILT} = \frac{2n}{n^2+1}\exp.^{-\alpha_t t} \quad (1)$$

where n is the real part of refractive index ≈1.72 for Sp; α_t is the total attenuation coefficient (including scattering and absorption); t the Sp plate thickness.

The maximal transmission of a spinel plate is ~87% in a wide wavelength (λ) range (0.25–5 μm). Below, specimens exhibiting an ILT ≥ 75% will be labeled as "highly transparent", those with an ILT in the 50–75% range – as "transparent", while "translucent" covers the 20–50% span.

As it may be seen, for ensuring high ILT the important tasks are the minimization of radiation scattering on heterogeneous phases ($n \neq n_{Sp}$) and of its absorption. A more detailed description of these tasks is given in the following subsections. The width of the UV-IR high transmittance window will be addressed in Section 2.1.4.

1.3.1. Porosity and other heterogeneities limitation

The cubic spinel has no birefringence (even the inherent birefringence, significant at λ < 200 nm, is ~0 for polycrystalline parts[6]), but may scatter radiation if it includes second phases exhibiting a refraction index different from that of the matrix [in the visible (VIS) range $n \sim 1.72$]. Porosity ($n \sim 1$) is the most

Table 2
Characteristics of high performance transparent spinel parts.

Developers (location and approach)	Characteristics					
	$\overline{GS}$	ILT (I) or TFT (T) %	$\overline{Hardness}$ GPa	$\overline{TRS}$ MPa	$\overline{E}$ GPa	Merit
IKTS – Dresden AS + HIP	0.35	84 (I) t = 3 mm	HV10 = 14.0–15.0	200–250	275	IxGS (<1 μm) xHVxmedium size (25 cm)
ICSI – Haifa AS + HIP	0.45	81 (I) t = 2 mm	HV5 = 14.0–14.5	180–220	290	IxGS (<1 μm)
TA&T – US HP + HIP	>50	83 (T)	HK0.2 = 16.4	210	280	Large size (L ~ 50 cm) × complex shape × uniform properties
NRL-MER – US HP + HIP	~25	82 (T)	16.0[a]	300[a]	280	Large size (L ~ 40 cm), complex shapes xT
Coors – US HP	>50	82 (T)	HK0.2 = 13	170	265	Early good performance
NIMS – Japan SPS	0.40	70 (T)	>15[a]	400[a]	–	Fast sintering

[a] Unusually high values; not consistent with microstructure.

Please cite this article in press as: Goldstein A. Correlation between $MgAl_2O_4$-spinel structure, processing factors and functional properties of transparent parts (progress review). *J. Eur. Ceram. Soc.* (2012), doi:10.1016/j.jeurceramsoc.2012.02.051

deleterious such phase. The pores scattering coefficient α_{Sp} is given by the relationship[11]

$$\alpha_{Sp} = \frac{Po}{(3/4\pi)(\phi_P/2)^3} C_{sp} \quad (2)$$

where Po is the percentage of porosity; ϕ_P is the pores diameter (in practice there exists a $\Delta\phi_P$) and C_{sp} the scattering cross section of one spherical pore.

After calculating the C_{sp}, using the Mie approach (the calculation was done for a matrix with $n = 1.76$), it was shown by Apetz and Van Bruggen[11] that both the ILT and the total forward transmission (TFT) are markedly affected by the characteristics of porosity. These results were confirmed by the more comprehensive (various "n" values) calculations reported[9] where a curve corresponding to the $n = 1.72$ applicable to spinel, is also given. The main factor of influence is the λ/ϕ_P ratio. Radiation scattering decreases when this ratio deviates from unity, as shown by Fig. 1a of Krell et al.[9] For decreasing optical loss to acceptable levels – by reducing pores size – the λ/ϕ_P ratio has to be at least ≥ 8. Thus, reducing pore size to under 40 nm ($\lambda/\phi_P \sim 10$) markedly decreases their scattering ability[9,16] of visible light, but even such small pores may contribute to transmission loss, especially if UV applications are considered.[9,17–20] When $\phi_P \gg \lambda$, average optical loss is once again reduced, but large pores are stress concentrators. The worst situation is $\lambda \approx \phi_P$. For $n = 1.76$ (Al_2O_3) the back scattering (not total) of a ~1 mm part – having a residual porosity of as low as 0.01 vol% ($\phi_P = 50$–100 nm) – is still ~2%.

The amount of porosity also influences transmission.[11,18] As it is clear from the above, the admissible Po is correlated with the pores size distribution. Practice shows that, considering the usual size distribution of the residual porosity in transparent spinel parts, one has to limit its volume fraction to $Po < 100$ ppm (and for some applications <10 ppm). Finding ways to produce parts of low enough porosity is the main challenge confronting transparent spinel development. Moreover, such porosity has to be achieved at temperatures low enough to limit the concentration of oxygen vacancies and the gray "color" such sites and/or other absorbers might cause (see Fig. 10 of Krell et al.[9] and further discussion here in Section 2.1.4.2). Such a task becomes really hard if the additional requirement of $\overline{GS}$ 3 μm (imposed by the mechanical properties) is added. The state of the parts in which $Po \leq 100$ ppm will be called below as "full densification".

It is also important to keep the parts free of radiation scattering ($n_S \neq n_{Sp}$), solid, second phases (crystalline or amorphous). Such phases may be carried by impure raw materials or introduced by processing tools (especially grinding media), being located along grain boundaries, at triple junctions or as micro or larger size, randomly distributed, defects.

1.3.2. Limitation of radiation absorbing centers content

Besides the nano/micro scale heterogeneities discussed above, atom scale impurities may also have a deleterious effect on optical transparency. The α_t, which appears in (1), also includes a component describing the influence of absorption (which obeys the Lambert–Beer relationship) on ILT.

In amounts higher than ~50 ppm, transition metal or rare-earth cations may negatively affect VIS or IR transmission owing to absorption, while in UV (important for applications like lithography) transmission may be deteriorated by as little as a few ppm.[6,17,18] Similar effects may be caused by certain oligo-atomic clusters (a term which here includes both small molecules and disordered assemblies of a small number of atoms) and also by point defects able to capture free electrons.[9,16,17] Therefore such centers need to be kept in very low concentrations.

1.4. Paper's objective and structure

For reaching the targets of research mentioned above in a way which uses minimal trial and error experimentation, it is important to develop a deep and comprehensive understanding of spinel's structure, from atomic to macro scale, and of the possible correlations between the structural features, the processing operations and the functional properties of the finished parts. Based on such an understanding the optimal correlations can be selected, i.e. efficient technologies can be designed within a reasonable timeframe. While certain issues are still open, considerable progress was made in about fifty years of technological research.

This paper endeavors first of all to give a critical review of this progress. Results presented in the literature or obtained in the author's lab (some of them published here for the first time) are used. It was tried to address as many as possible of the relevant issues. The data presented are discussed, mainly, from an engineering perspective. Certain suggestions on how to improve current practice, based on the more recent research results, are also offered, together with notes on topics requiring additional research.

2. Structural characteristics (atomic to macro scale) with influence on transparent spinel fabrication. Their correlation with processing

"High" levels of densification are required by many types of ceramics, like those used for electronic, prosthetic or high wear resistance parts. In such cases residual porosities in the 0.1–1.5% range are acceptable. Really high densification levels, i.e. the need to ensure reduction of porosity to under 100 ppm, are specific, however, to technologies for transparent spinel (or other transparent ceramics) obtainment.

Some guidance on which are the most relevant characteristics one needs to control in order to achieve full densification – was provided, even for early efforts, by the general relationships governing various aspects of the densification process. For instance, from the relationship (3)[21] the necessity of ensuring low particles and pores size, together with high surface energy, for maintaining a high drive for sintering, is seen.

$$\sigma_S\,[\mathrm{MPa}] = \frac{2\gamma_{sV}}{r} \quad (3)$$

where σ_S is the sintering stress; γ_{sV} is the surface tension (it is ~1 J/m^2 for oxides similar to Sp[21]); r the radius of pores or powder particles.

Please cite this article in press as: Goldstein A. Correlation between $MgAl_2O_4$-spinel structure, processing factors and functional properties of transparent parts (progress review). *J. Eur. Ceram. Soc.* (2012), doi:10.1016/j.jeurceramsoc.2012.02.051

The equation describing the kinetics of the process (its advanced stages) (4)[22] shows the importance of raising "good" diffusion rates [$D_{b,L}$ (as opposed to surface diffusion, D_S, which helps grain growth)]. Eq. (4) (or similar) also shows the usefulness of a low grain size, which controls the pores length (intermediary stage) and their spacing after pinch off (final stage).

$$\frac{d\rho}{d\tau} = 31.5\frac{V_M}{kT\overline{\overline{GS}}^2}(1-\rho)\left[D_L + \frac{\pi\delta_b D_b}{\overline{GS}}\right]P \quad (4)$$

where ρ is the density; τ is the time; V_M is the molar volume of diffusing species; D_L is the lattice diffusion coefficient; δ_b is the grain boundary width; D_b is the grain boundary diffusion coefficient; and P the pressure.

As it will be shown below (chapter 2), the technologies put forward – especially during the last 15 years – improved, bringing toward optimal, the value of the parameters mentioned in (3) and (4), by the aid of adequate processing operations especially at the nano/micro level.

However further progress is needed and possible. The significant degree of influence of certain other factors [not carried by (3) and (4)], like initial pores size distribution and its dynamics, pores topology in the final stage of sintering (see Section 2.2.2) or the agglomerated state of nano-powders, was realized more recently. Processing improvements, for which the effect of such factors is taken into consideration, are under development; applied early versions have already been able to reduce grain size into the submicron range while preserving transparency.[10,16,23] Recent progress also allowed a more complete identification of the characteristics influencing radiation absorption and ways to control them.

2.1. Atomic scale (1–10 Å)

Some of the characteristics mentioned above concern the ionic lattice; those are addressed in this section while those concerning the nano/micro scales are discussed in Section 2.2; macro scale issues are treated in Section 2.3.

2.1.1. Influence of magnesium aluminate ($MgO{\cdot}xAl_2O_3$) lattice intrinsic characteristics on sintering

The lattice of spinel is a very slightly distorted cubic one, being usually described by the space group $Fd\bar{3}m$ (no. 227 in IT), or more accurately, by SG $F\bar{4}3m$.[24] Some of its inter-dependent characteristics – such as distortion pattern and level, point defects type, concentration and mobility – influence ionic diffusion and, as a consequence, the sintering process. The lattice configuration is affected by many factors, including: powder preparation conditions, impurities, sintering atmosphere, thermal treatment schedules, electromagnetic fields, irradiation, etc.; an additional factor specific to spinels is the inversion degree. Inversion is a term describing the fact that a fraction of the Al^{3+} ions occupy sites – exhibiting a tetrahedral coordination by O^{2-} – which in an ideal, fully ordered, lattice are reserved to Mg^{2+}. As a result, $Al_{Mg}^{\bullet}$ type point defects are formed. The ratio of $[Al_{Mg}^{\bullet}]/[Al] = i$ is the "inversion parameter" $\{i \in [0–1]$; for synthetic spinel $i \in (0.2–0.8)\}$. It is considered that such defects are compensated, electrostatically, by Mg'_{Al} (i.e. $[Al_{Mg}^{\bullet}] = [Mg'_{Al}]$), but, depending on conditions, other neutralization schemes, involving larger sets of point defect, may be thermodynamically preferred. When the thermodynamic conditions are modified, the three degrees of freedom of the lattice [the lattice parameter (a), the "i", and the repeat unit of the anions sublattice (u)] are used for rearrangement, so as to attain the lowest energy configuration in the given set of conditions.[24]

The information available on the various characteristics of the lattice, and their correlation with diffusion, comes from measurements of diffusion coefficients, computer simulation of lattice behavior and interpretation of sintering results.[24–45] The real lattice is a very complex system. An example may illustrate this. Both the O_i'' and the $V_o^{\bullet\bullet}$ type of defect help oxygen's diffusion. It does not necessarily mean, however, that anion diffusion rate will increase in proportion to the concentration of the individual defects. As a result of a change in sintering conditions some of the $V_o^{\bullet\bullet}$ s may capture interstitials, or only trap them, depending on their relative positions; in both cases mobility is reduced.[30] The ratio between the mobility of the two defects is not always the same.

Despite the fact that the available data offer a still fuzzy image of the lattice structure, its examination is able to facilitate the understanding of certain aspects of the sintering process, as shown below.

For instance, ions self-diffusion rates measurement suggests that the most important types of defect are those related to the anion, i.e. the oxygen interstitial O_i'' and the oxygen vacancy $V_o^{\bullet\bullet}$ (using the usual Kröger–Vink notation). In the case of Mg-spinel, the slowest ion is the O^{2-} anion $\{D_O(O^{2-}) \approx 10^{-4}$ m^2/s, while for the cations $D_O \approx 10^{2-}$ m^2/s[31]$\}$. The activation energy (Q) for O^{2-} diffusion (~400–500 kJ/mol) is similar to that of the general densification process (Q = 430–490 kJ/mol), a result which lends further support to the view that the anion diffusion controls the sintering rate.[31] This view is currently universally accepted.[8] Recent simulation work, however, suggests that Al^{3+} might be, in certain cases, the slowest ion.[30]

The diffusion of O^{2-} seems to take place mostly by the aid of vacancies, despite the fact that the interstitials (O_i'') migrate faster.[30] In spinel the oxygen interstitials are of the split type, aligned with a $V_o^{\bullet\bullet}$ along $\langle 1\,\bar{1}\,0\rangle$. The effect of the vacancies is expected to be stronger, despite their lower mobility, because the $[O_i'']$ is, in most conditions, supposed to be much smaller than $[V_o^{\bullet\bullet}]$.

The composition, qualitative and quantitative, of the point defects population (including $V_o^{\bullet\bullet}$) varies as a function of a number of parameters, like, for instance, the value of the $[Al_2O_3]$:[MgO] (X) ratio. This is of practical importance because single-phase spinels of various X can be obtained despite the fact that the thermodynamic diagram, of the MgO–Al_2O_3 system, indicates only the stoichiometric (X = 1.0) material as stable at RT. In reality, owing to kinetic reasons, solid solutions with the X varying in a wide range (0.7–7.0, according to some[29]) are also stable at low temperature. Possible, qualitative compositions of the point defects population – for spinels exhibiting various "X" values – have been put forward (based, though, on the incomplete information available on lattice structure). Quantitative treatments were also attempted,[32] but considering how

Please cite this article in press as: Goldstein A. Correlation between $MgAl_2O_4$-spinel structure, processing factors and functional properties of transparent parts (progress review). *J. Eur. Ceram. Soc.* (2012), doi:10.1016/j.jeurceramsoc.2012.02.051

little solid knowledge exists on the interaction patterns of the multi point defect systems, existent in a real spinel lattice, such endeavors seem premature. Here the set of defects proposed by Y.M. Chiang and W.D. Kingery and the potential consequences of their existence on densification and grain growth rates, is given,[33,36] in order to illustrate the type of predictions such a correlation allows. According to these authors, for $X<1$, in the case of the grains cores, the main point defects are $V_o^{\bullet\bullet}$, $Mg_i^{\bullet}$, $Al_i^{\bullet\bullet\bullet}$ and Mg'_{Al}. At the grain boundaries, however, the Al/Mg ratio increases, and the dominant defects become $Al_i^{\bullet\bullet\bullet}$, V'''_{Al}, Mg'_{Al}. For $X\geq 1$ the bulk includes $Al_{Mg}^{\bullet}$, V'''_{Al} and V''_{Mg}. The increase in Al/Mg ratio in the grain boundary region occurs also for $X\geq 1$ compositions. So, for $X\geq 1$ at grain boundary the defects are $Al_{Mg}^{\bullet}$, O''_i, V''_{Mg}, and V'''_{Al}. The actual point defects existent at a given "X" are also influenced, of course, by aspects like the inversion process and sintering atmosphere composition. The inversion, for instance, introduces (or modifies) the concentration of Mg'_{Al} and $Al_{Mg}^{\bullet}$ type defects. It does not directly modify $[V_o^{\bullet\bullet}]$ as long as defects pairs form. By creating quite deep energy traps, on certain sites, inversion may affect indirectly the oxygen vacancy concentration too.[30] Compensation of $Al_{Mg}^{\bullet}$ by O''_i and of $[Mg'_{Al}]$ by $V_o^{\bullet\bullet}$ is also a possibility.

From the above it would appear that a $X<1$ is advantageous for densification. The $[V_o^{\bullet\bullet}]$ concentration increases in this region (thus improving anion diffusion) and, as a result, densification rates (in the intermediary and most of the final stage) should indeed increase. However, in the case of transparent spinel, this benefit may be offset owing to the simultaneous increase of grain growth rates. The deleterious effects of coarsening are felt, mostly, at the very end of the final stage (the most problematic segment); grain growth increases both pores size and occlusion probability. It was shown in Refs. 33,36 that for $X<1$ the grain growth rate is dramatically raised (owing, mostly, to the specific point defects populations present) compared to the $X\geq 1$ domain. It is therefore likely that the strong negative effect on grain growth outweighs the benefits to diffusion (and thus densification rates) brought by the favorable point defects composition. Experimental sintering tests are needed in order to determine which effect is stronger. Looking, now, to the defects present for "X" ≥ 1, both in the bulk and at grain boundaries, it can be seen that variation of stoichiometry, in this range, is not directly affecting the $[V_o^{\bullet\bullet}]$. The grain growth is much slower when $X\geq 1$ than in the case of $X<1$.[33,36]

Recent experimental work shows that variation of X, in the $X=1.0$–3.0 range, affects sintering in a rather complex manner.[37] While X varied from 1.5 to 3.0, an increase in sinterability was observed after a decrease in the $X=1.0$–1.5 range. This is explained by the fact that in this region a spinel + corundum phase system appears. An increase in oxygen diffusion rate, for $X>1.0$, was reported by K.P.R. Reddy and A.R. Cooper.[25] It may be that the presence of O''_i –which form at the grain boundaries when $X>1$ – explains, at least in part, together with the phase composition modification, these observations. The results of[37] show that besides the modification of the lattice, the variation of X affects sinterability also through other aspects, like phase composition variation. The number of publications regarding the effects of "X" on processing and properties is rather small, e.g. Refs. 37,46–50.

Simulations showed an interesting effect, with significant consequences on the way point defects affect properties and/or diffusion. In MgO, for instance, interstitial clusters (anion + cation) migrate faster, in a way different from the components.[40] In spinel clusters seem immobile but tend to act as nuclea for larger defects formation.[30] Clustering, especially trimers, of charge compensating defects, is favorable (energetically), more than in other lattices, with the antisite defects, produced by "i", raising the probability of the process. Some dimers (without antisite components) also show high binding energy, albeit less high than trimers (for the former configuration entropy loss is more significant). Large size lattice defects, like dislocations, are not addressed here; their effect on densification seems to be less important than that of point defects, except situations in which high pressure is used.[31]

2.1.2. Extrinsic point defects effect on sintering

Any real spinel lattice includes impurities. Their effect has to be considered too in addition to that (dominating) of the intrinsic ones. Most of the Sp lattice impurities tend, in order to minimize elastic energy and/or effectuate electrostatic compensation (maybe also other reasons), to massively segregate towards surfaces, including grain boundary regions. This essentially affects the way these ions exert their influence. Compelling evidence for the segregation process is already available. The work of G.B. West et al.[38] showed that this is the case for a number of lanthanide cations, while Y.M. Chiang and W.D. Kingery have done the same for elements such as Si, Ca or S.[36] The latter authors (1989) considered that the influence of the segregates is minor, at least on grain growth. However it was shown by recent work[39] (for the case of YAG but also actual for Sp) that segregation drive depends significantly on surface crystallography. Segregated solutes affect, inter-alia, the γ_{sV},[8,43] (sintering drive is sensitive to segregants) with this dependence being modulated by the type of planes making up the surfaces.[39] Moreover, in a study (still underway, at ICSI) we observed that even addition of low amounts of transition element cations containing oxides (80–250 ppm range) has a strong deleterious influence on densification. It is not yet clear how much of the additions entered the lattice and what fraction operates as a second phase. Solutes affect also grain boundary mobility[51–53] and, as a result, also pores topology. These examples suggest that transition ions (segregated at grain boundaries) may influence, more than initially thought, by various mechanisms, both densification and grain growth. It is yet premature to draw general conclusions on the way segregates affect spinel's sintering.

The complexity of the issue (i.e. influence of extrinsic ions) can be further underlined by considering the effect of LiF addition to spinel sintered by pressure assisted firings. This additive – introduced, for Sp, by W.H. Rhodes (sixties) and made popular by D.W. Roy[5] – has a number of useful effects (lubricant, carbon scavenger) and is used in most of the hot pressing (HP) procedures today.[31,54–57] Moreover, it was proposed by I.E.

Please cite this article in press as: Goldstein A. Correlation between $MgAl_2O_4$-spinel structure, processing factors and functional properties of transparent parts (progress review). *J. Eur. Ceram. Soc.* (2012), doi:10.1016/j.jeurceramsoc.2012.02.051

Reimanis et al.[56] that, in the presence of LiF, a defective spinel re-precipitates, from an oxyflouride melt formed (850–1000 °C) by interaction of LiF with spinel, on regular spinel cores, according to: $3LiF \xrightarrow{Sp} Li'_{Mg} + 2Li''_{Al} + 3F_O^{\bullet} + V_O^{\bullet\bullet}$. The defects thus formed, especially $V_o^{\bullet\bullet}$, are able to promote O^{2-} diffusion at the peak HPing temperatures (≥1550 °C). Such an additional effect of LiF may significantly enhance sintering in the last stages, explaining the observed reduction of activation energy from ~480 kJ/mol for pure spinel down to ~200 kJ/mol for LiF–$MgAl_2O_4$ (hot pressed).[56] A highly uniform distribution of the additive is important to fully exploit its abilities.[57]

2.1.3. Oligo-atomic clusters influence on sintering

During sintering various species of oligo-atomic clusters move along the grain boundaries, with important consequences on densification (and other processes). This term covers here both small molecules and assemblies of a few atoms (like, say, carbon); they may be neutral or charged. For instance, the out diffusion – from closed pores – of O_2 and N_2 (low diffusion rates in oxide lattices) is essential for advanced densification during sintering in air (AS). Gas trapped in the closed pores generates a pressure (high at T°_S) opposing densification. This out diffusion process, difficult to complete in air, makes further progress during hot isostatic pressing (HIP), which occurs under Ar. As far as the negative effect of trapped gas is concerned, effectuation of the first stage of sintering under vacuum (VS), is advantageous (no gas in pores) on the condition that it is done at temperatures where the evolvement of Mg or the generation of vacancies (that cause absorption) (both favorized by vacuum, as further discussed in Section 2.1.4.2) is negligible.[34]

In the case of VSed parts, further subjected to HIPing, Ar coming from the HIP atmosphere (at ~200 MPa) can reach the closed porosity. Ar can be trapped also if open porosity left by AS is closed during HIPing.

Individual carbon atoms, oligo-atomic clusters or larger particles are, in some cases, present in Sp parts that have been subjected to HP (spark plasma sintering – SPS) or HIP (possible formation mechanisms will be discussed in Section 2.1.4.2, dealing with effects of carbon on radiation absorption). Here it is only noted that a number of processes – including chemical reaction, dissolution (mostly in the grain boundary region) into the lattice, reduction of boundary mobility (M_b) – may occur, when carbon is present, and affect the interrelated grain growth and densification[8]; data available does not allow a detailed discussion of this issue yet.

2.1.4. Point defects and oligo-atomic clusters influence on radiation absorption

For ensuring high transmission, absorption loss of a transparent spinel part has to be also strictly controlled, like the scattering on pores. The band gap of pure poreless spinel (at ~8 eV[58]) is large enough to put transmission cutoff at a λ as low as ~170 nm. The "window" limit, at high wavelength ($T \sim 70\%$ at $\lambda = 5$ μm; $t = 4$ mm), is set by the lattice vibrations (highest energy phonons). A number of local electronic systems – able to cause absorption within this window – may appear in practice and significantly affect transmission. These systems are briefly discussed here.

2.1.4.1. Transition and rare-earth cation impurities. Such ions, if present in the lattice (mostly at grain boundaries), may affect transmission in a wide spectral range, from the UV cutoff down to frequencies near the MIR edge of the window. However, with a few exceptions (Ni^{2+}, Co^{2+}), the d–d or f–f type transitions, which generate bands in the VIS and IR, are weak (orbitally forbidden), so that only at relatively high concentration they pose a problem. High concentrations are not frequent, because current powder preparation methods ensure high purity. Lanthanide impurities appear in even lower amounts than the d-ions. Furthermore, solubility of most such ions seems to be very low in the Sp lattice. However this type of impurity, even in the low amount they appear in, is deleterious for applications in which the UV domain is relevant. There, much stronger bands, produced by charge transfer transitions, are present; even a few ppms may pose a problem in such cases. Certain ions, like Cr^{3+} seem able to improve mechanical properties,[42] but owing to the pre-eminence of optical properties, they are still viewed as deleterious impurities.

2.1.4.2. Carbon single atoms, clusters and $V_o^{\bullet\bullet}$. When sintering stages are performed in oxygen lacking atmospheres, shades of gray to black "color", of variable intensity, appear. This effect is stronger when carbon containing elements are present in the heating enclave, with its intensity significantly dependent on the carbon release "ability" of those elements. In the case of thick parts ($t > 2$ mm) a coloration intensity gradient exists, with a reduction toward the median plane of the plate. These undesired hues markedly reduce optical transmission (see Fig. 1, gray-black curves set). They can be eliminated, usually, by annealing in air (Fig. 1 set of colorless curves). As far as the temperature required (depends on color intensity) is low enough to avoid reformation of pores, the annealing does not cause loss of transparency. The most likely causes for these hues are either carbon atoms (individual or clusters) or oxygen vacancies, or both. There are "symptoms" suggesting the presence of both.

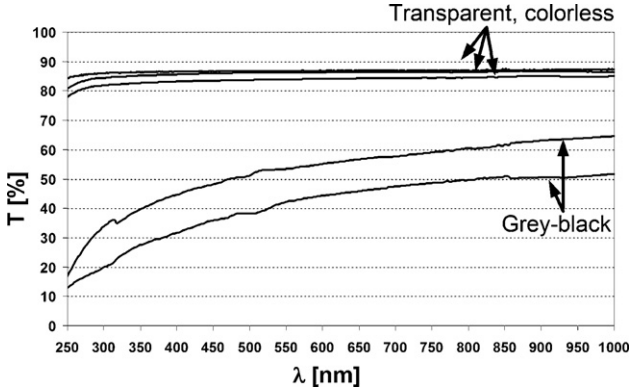

Fig. 1. Optical transmission spectra of transparent spinel specimens ($t = 2$ mm; polished) obtained (ICSI) by AS + HIP. Colorless (three upper lines): after post HIP annealing in air (1100 °C/5 h). Gray-black (lower two curves): as HIPed (polished) state.

Please cite this article in press as: Goldstein A. Correlation between $MgAl_2O_4$-spinel structure, processing factors and functional properties of transparent parts (progress review). *J. Eur. Ceram. Soc.* (2012), doi:10.1016/j.jeurceramsoc.2012.02.051

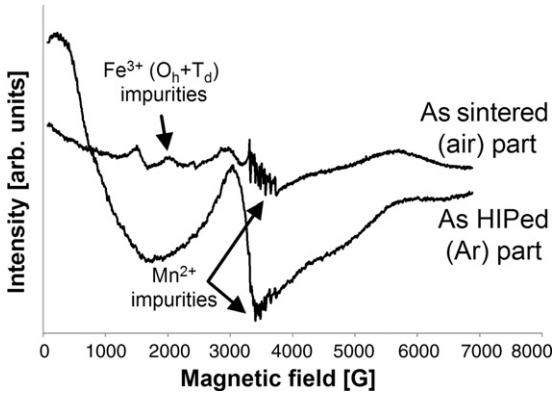

Fig. 2. EPR spectra of un-doped transparent spinel specimens (X-band, RT). As sintered (air) specimen: white, slightly translucent. As HIPed (Ar) specimen: highly transparent; light-gray tint (strong signal at ~3500 G, probably from V_O or $V_O^{\bullet\bullet}$ type absorptive clusters).

The profile of the optical spectra (see curves in Fig. 1; gray-black set) is consistent with a situation in which a strong absorber and a source of scattering are simultaneously present. This may happen in the presence of carbon colloidal particles or much smaller clusters (molecular size) associated with some residual porosity. On the other hand, electron paramagnetic resonance (EPR) examination of HIPed specimens (see Fig. 2) strongly suggests the presence of $V_o^{\bullet}$ and/or V_O color centers [A. Goldstein, A. Stevenson, unpublished results]. The profile and position of the major signal are very similar to ones attributed to V_O.[59] Such defects are present in oxygen scarce atmospheres, owing to:

$$O_O \Leftrightarrow V_O^{\bullet\bullet} + \frac{1}{2}O_2(s) + 2e'$$

where

$$[V_O^{\bullet\bullet}] = \frac{K_n}{n^2 \cdot P_{O_2}^{1/2}} \quad (5)$$

P_{O_2} = partial pressure of oxygen; $n = [e']$. They may also be responsible for the colors seen. The V_O or $V_o^{\bullet}$ are a result of $V_o^{\bullet\bullet}$ entrapping the electrons released by O_O. Only if other very favorable electrostatic compensation options are available, is there no electrons trapping. The V_O type centers alone, though, cannot explain the profile of the optical spectra like those in Fig. 1. Such defects, being localized electronic systems, can produce only discrete absorption bands, with a more or less Gaussian profile.[19] Spectra of specimens which surely include color centers (irradiated) do show the expected local bands[41]; interaction between $V_o^{\bullet}$ and V_O clusters would generate an envelope one can resolve into Gaussian components. Even the envelope produced by a larger set of color centers cannot generate transmission curve profiles like those observed.

A possible conclusion, consistent with both the optical and EPR data, is that both carbon clusters and oxygen vacancy based point defects are present, but the former dictate the overall spectral curve profile. For the case of HP (SPS)ed parts, the presence of carbon inside the parts was observed and can be explained easily. The parts are in a porous state at the start of the sintering. If the graphite parts release true carbon particles (this depends on the state of the graphite parts) they will be trapped within the pores. In fact, G. Bertrand-Granger and colleagues[60] were able to detect such particles and even to reproduce the transmission curve of a SPS spinel part by a calculated one (assuming the presence of porosity + graphite particles). The presence of carbon in HPed or SPSed parts has been, indirectly, proven also by S. Meir et al.[55] and I. Reimanis et al.[8] In Ref. 55 it was also shown that LiF, besides its effect on sintering, may also help in "cleaning" the parts subjected to SPS based on the reaction $n\mathrm{LiF} + n\mathrm{C} \rightarrow n\mathrm{Li} + (\mathrm{CF})n\uparrow$.

If carbon is admitted as a color source in HP (SPS)ed parts, it is very tempting to consider this source also in the case of HIPed parts, especially because they have similar transmission curves. In the case of the latter, though, it is more difficult to understand the way carbon appears inside the parts; the specimens subjected to HIPing are without open porosity. The diffusion of CO molecules or individual carbon atoms along the grain boundaries may provide an explanation. The fact that inside – along its grain boundaries – a spinel part, subjected to HIPing, a strongly reductive atmosphere prevails, is demonstrated by a simple experiment. An air sintered part doped with copper shows the greenish-blue color proper to Cu^{2+}. After HIPing the initial color changes, first to lack of color (Cu^{+}) and then to red (Cu° clusters) as the HIPing temperature is increased, indicating a progressive reduction of Cu^{2+}. A strong reductor, able to interact (redox) with Cu^{2+}, must be present. CO is presumed to be present in the atmosphere of HIPing machines[9] or it may form at the carbon coating/spinel interface. Carbon may re-form then, inside the part, from the CO diffusing along grain boundaries, according to: $2\mathrm{CO} = \mathrm{C_S} + \mathrm{CO_2}$. Spinel structure oxides are known to be good catalyzers for reactions which extract solid carbon from its gaseous oxides.[61] If this sequence of events occurs, the reaction product has to take the form of the oligo-atomic clusters owing to the limited space available. Another possibility is the slow diffusion of carbon single atoms, along the grain boundaries, from the macroscopic surface toward the inside zone of the specimens. The as-HIPed parts exhibit, often, black, opaque thin coatings, in which we clearly detected the presence of C by EMPA (SEM). Such coatings are an efficient carbon source; after removing the coatings, the black hues remain with the color intensity decreasing markedly from the specimen's surface toward its middle plane.

In both cases the size of the carbon impurities has to be close to that of atoms; this may explain the failure of TEM to detect such units. If carbon really exists in the HIPed parts, it also seems to be present in very low amounts. Preliminary explorations – by ToF-SIMS, XPS or NMR, failed to detect its presence.

It results from the above that, especially for the case of HIPed parts, firm identification of the gray coloration cause(s) still needs further work.

2.1.4.3. Sulphur. A task more easily accomplished was the identification of the origin of the yellow tint (its intensity also, usually, decreases toward the middle plane of the thickness) that sometimes accompanies or even dominates the gray hues discussed above. It became apparent to us, recently, that such tints appear only when powders derived from sulphates are

Please cite this article in press as: Goldstein A. Correlation between $MgAl_2O_4$-spinel structure, processing factors and functional properties of transparent parts (progress review). *J. Eur. Ceram. Soc.* (2012), doi:10.1016/j.jeurceramsoc.2012.02.051

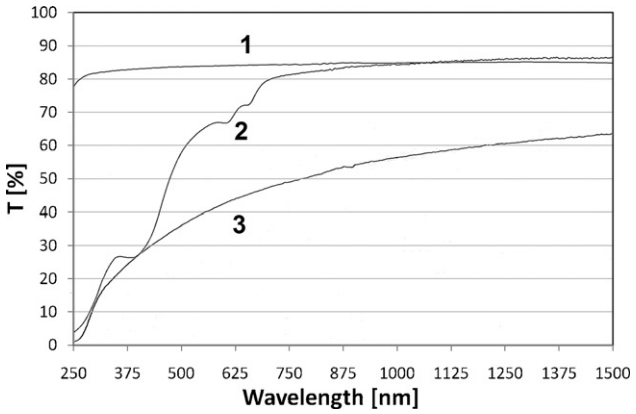

Fig. 3. Optical spectra of transparent spinel specimens ($t = 2$ mm; polished). (1) Colorless highly transparent part (AS + HIP). (2) Yellow tinted transparent part (AS+HIP), derived from powder including sulphate. (3) Low transparency, colorless (includes many white opaque spots). (AS 1380 °C/3 h; no HIP); derived from SN2.

used. Sulphate anions can enter (moderate concentrations) the lattice of oxides like spinel by substituting O^{2-}. In air they remain stable up to high temperatures [like those prevalent at $T°_S$ during the AS stage (when an AS + HIP approach is used)]. In Fig. 3 curve 2 the optical spectrum of a transparent disk, exhibiting a yellowish, slightly gray, hue, is given. Analysis of the curve (based on 62) clearly shows that it is generated by the presence of S_8 molecules. The sulphur molecules result from the reduction of the sulphate during HIPing. The yellow tint can be always (i.e. even if intense) eliminated by annealing in air ($S_8 \xrightarrow{O_2} SO_2$) but bubbles may form if the required temperature is too high (over ~1250 °C) owing to high color intensity (the intensity increases with HIPing temperature).

While strong yellow tint seems to require the presence of sulphur, lighter coloration may be caused, in principle, also by other mechanisms. For instance, certain scattering loss curve profiles cause stronger transmission reduction in the violet-blue region, favoring yellow-orange hues formation. Moreover, the most intense d-d type bands [$^4A_1$, ^4E (G) and $^4T_2$ (G)] of Fe^{3+} are located, for oxides like Mg-spinel, in the same region. For the d^5 type Fe^{3+} ion, the ground state is such ($^6A_1$) that the bands are also spin-forbidden and, as a result, very weak.[19] Certain yellow sapphires owe their color to these Fe^{3+} d–d bands; the cation is present though in significant concentrations (up to 1%). At high concentrations of Fe^{3+} the tails of the strong charge transfer bands (located at $\lambda \leq 250$ mm) can extend into the visible domain, adding to the absorption of the d–d bands.[19] Similar effects are possible also in spinel if enough Fe is present, but most of the powders used for transparent parts fabrication include less than 50 ppm of Fe. This is not enough to generate perceptible coloration; it is enough, however, to cause significant absorption in the UV (180–350 nm range). The fact that the yellow tints loose intensity when the specimens are heated in O_2 containing atmospheres (e.g. air) is additional evidence showing that the color is not caused by Fe^{3+}.

2.2. Nano/micro scales (10 nm–100 μm)

The structure, at these scales, of the spinel particulates and bulk bodies (green and in various stages of the sintering process), has a marked effect on the properties of the finished parts. As far as optical transmission is concerned, structural features – at this scale (especially porosity) – seem to be the most important aspect within the set of factors which influence this property. Correlation of structure at these scales with processing is discussed in this section.

2.2.1. Powder and green body structure

The fact that the configuration of the green body affects Sp sintering was taken into consideration already in the early works.[1,4,5] How important this aspect is, however, was only gradually understood.[16,18,23,63,64]

2.2.1.1. Structural requirements for sinterable green bodies. How strong is the influence of the green body nano/micro scale structure (especially the pores size distribution, measurable by mercury intrusion) and its long range uniformity on the advanced sintering of spinel was demonstrated only recently, mostly by the work done at IKTS Dresden.[16,17,63] The need to consider the contradictory effects of lowering crystallites size under a certain limit (variable from ceramic to ceramic), was stressed. It was also shown that by control of the pores size distribution width, the sintering temperature may be drastically reduced.[10] Some further discussion of the topic is attempted here.

For this let us first briefly recapitulate, by the aid of the schematic in Fig. 4, which are the desired features of a green body derived from agglomerated powders. These features are suggested by some simple requirements of densification thermodynamics, kinetics, and transparent spinel sintering practice. For a high sintering drive the crystallites need to be as small as possible, and so do the pores. The size distribution of both has to be narrow. Owing to the extremely low final porosity volume necessary, the most relevant is the maximal, not the average, size. Were the crystallites spherical, monosize and not agglomerated (a state not yet achieved in commercial spinel fine powders) – ordered arrangements like those in Fig. 4a (or more compact) could have been obtained, by suitable forming. In such a structure pores can be more than five times smaller than the crystallites, and exhibit a very narrow size distribution. In the case of silica we have observed that such a structure (even for "large" particles 1 μm in size) allows massive reduction of sintering temperatures.[65] Considering these results for 50 nm

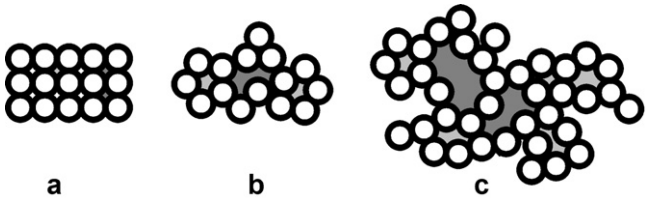

Fig. 4. Schematic representation of crystallites (represented as small circles) packing pattern in a green-body. (a) Ideal state. (b) State attainable, in practice, by optimized processing. (c) State resulting from poor processing (does not allow attainment of full densification).

Please cite this article in press as: Goldstein A. Correlation between $MgAl_2O_4$-spinel structure, processing factors and functional properties of transparent parts (progress review). *J. Eur. Ceram. Soc.* (2012), doi:10.1016/j.jeurceramsoc.2012.02.051

spinel monosize spherical crystallites – exhibiting a compact (bcc or fcc) ordered arrangement – pressureless sintering temperatures not higher than ∼1100 °C would be expected to suffice for the attainment of a fully dense state. The real spinel green bodies are, however, collections of agglomerates of various size and shape, exhibiting internal, variable size, porosity. Only a small fraction of individual crystallites exists. Therefore, arrangements like in Fig. 4a are not obtainable in practice. A configuration like that in Fig. 4b would be a realistic target, allowing satisfactory densification under 1400 °C, while a state like in Fig. 4c would make full densification unattainable. In real compacts most of the largest pores are of the inter-agglomerate variety (Fig. 4b) and thus they represent the main concern. Moreover, while the intra-agglomerate pores size decreases rapidly, the inter-agglomerate ones tend to grow, in the first stage of sintering, due to the differential shrinkage of the agglomerates.[66] Therefore it is critical to keep the ratio between inter and intra-agglomerate pores as small as possible. It is also important to note that after the closure of their internal porosity, the agglomerates (particles) take the place of the crystallites as pore coordinating units.

Of course, in order to keep the densification process going, while new grain boundary is created, thermodynamics requires, in all stages of sintering, the maintenance of sufficient surface energy. This translates into the necessity of maintaining pore coordination (by the particles) numbers (NC) lower than a critical value NC_C.[66] The NC_C increases with size, so that particles size growth, while undesired, helps at least in reducing pore stability. The worst configuration is that in which large pores are limited by small particles. The necessary configuration has to be provided in the green state; unsuitable green configurations tend to become worse during sintering.

A high green state density BD_g (i.e. low Po) is also important, but useful only if it is achieved without impairing the features mentioned above; otherwise it may be even harmful. For instance, improving packing efficiency by using variable size particles, which are porous agglomerates themselves, is deleterious for densification (owing to differential shrinkage effects).

Critical and very difficult to achieve is the maintaining of suitable nano-microstructures in a homogeneous manner throughout the whole volume of the part. As will be detailed below (Section 2.2.2, discussing sintering) it is enough that a few percent of the green body volume – present in the form of relatively small (50 μm to 1 nm in size) discrete zones randomly distributed – have a non optimal nano-structure to make high transparency unattainable – at practically usable levels of thickness (≥2 mm).

2.2.1.2. Processing allowing the forming of easily sinterable green bodies. In order to obtain highly sinterable green bodies, first, suitable powders need to be selected. The complete set of features a suitable powder has to possess is an issue yet under debate,[5,10,16,17,64] therefore currently such a selection can be made only by the aid of tedious trial and error work. It would be very useful for one to be able to make a choice based only on analysis of a raw material's measured characteristics.

All powders need to be processed before forming; the processing varies markedly with their characteristics and the requirements of the forming method used. The sinterability of as-received powders can be significantly modified in this stage.

High purity, nano (refers to crystallite size), but agglomerated Sp powders can be obtained, today, by a wide variety of methods: co-precipitation, sol–gel, colloid/solution reaction, flame spray pyrolysis, decomposition of alkoxides under hyper-critical conditions, hydrothermal synthesis, nitrate melts cooling, etc. (e.g. Refs. 67–70).

In most cases forming is done by pressing, but procedures using suspensions in liquids (minimize re-agglomeration after milling)[71] like pressure slip-casting, gel-casting, pressure filtration or ultra-centrifugation were also examined, especially for complex shape parts. Such methods, though, are very difficult to apply in the case of the powders based on crystallites <100 nm,[16] the ones of most interest.

Agglomerates formation is the main cause of low sinterability. Agglomerates form because during powder synthesis temperatures in the 700–1200 °C (or higher) are attained. As a result incipient sintering necks form. The van der Waals (mostly the part owed to the London dispersion force) attraction, despite its low range, is also relevant, especially in the dry state of the raw material where the probability of inter-particles contact is high. Inter-particle bonds form also due to absorbed (small amounts) of water and organics. Comminution of the as-received powders by vigorous milling (or other methods, like rapid expansion in supercritical conditions or exposure to intense ultrasound waves) allows marked agglomerates size reduction (even sintering necks can be broken). Depending on its agglomeration pattern each powder needs a specific comminution program. Powders quite different in the as-received state can be brought to a similar fine state if suitably milled. The main problem is to achieve the desired level of comminution without introducing impurities. Agglomerates breaking is crucial, but is not always sufficient. Many of the bonds broken during comminution remain in that state, and yet, during drying of the suspension used for de-agglomeration and, even more, during pressing, a complex process of agglomerates re-forming also occurs (along with further breaking events). Bridges formed by water or organics, van der Waals forces, and, possibly, even "cold sintering" (the sintering stress for nano-size Sp particles may be higher than 200 MPa, and external compressive forces, active during forming, add to that) are responsible for re-agglomeration. Owing to these processes, the size distribution, shape and internal porosity of the particles – in the green body – are significantly different from what they were in the loose state of the as-received raw material. The flow of the granules, the shape, size and internal porosity of the fragments (generated by granules breaking) depend both on the characteristics of the raw material and the granulation conditions. Both the granules and the fragments (=smaller agglomerates) – under the action of the compressive force – change their position and structure continuously. If strong surface interaction operates, a number of small agglomerates or even individual crystals may lock to each other, defining among them large new pores. While the structure of raw material agglomerates is well studied,[66,71–76] the

Please cite this article in press as: Goldstein A. Correlation between $MgAl_2O_4$-spinel structure, processing factors and functional properties of transparent parts (progress review). *J. Eur. Ceram. Soc.* (2012), doi:10.1016/j.jeurceramsoc.2012.02.051

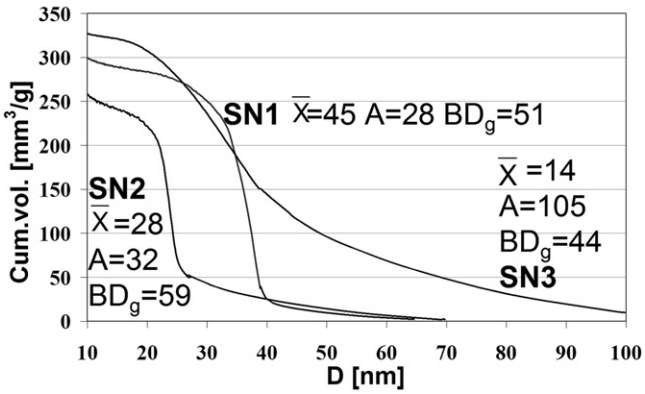

Fig. 5. Pores size distribution of green powder compacts (strengthened by heating to 900 °C/2 h) derived from spinel powders SN1, SN2, SN3. *D*: pores size; $\overline{X}$: average crystallites size [nm]; *A*: specific surface area [m^2/g]; BD_g: green bulk density [%TD].

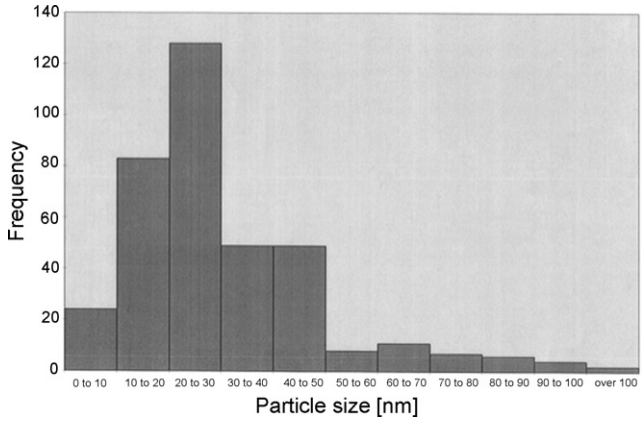

Fig. 7. Histogram of the crystallites size distribution of powder SN1.

effects of re-agglomeration are often overlooked, despite their significant influence on the pores size distribution and particles arrangement compactness, in the formed green body.

Some of the actions used in the powder processing and forming procedures already developed contribute to the limitation of the negative influence of re-agglomeration. So does, at the macro scale, the preparation of granules allowing good flow but which are also soft enough to breakup into small fragments easily and fully and exhibit a homogeneous internal structure and bonds strength. The use of non-aqueous suspending media during milling (reduces bonding of particles by the molecules of the liquid), dry storage atmosphere, low organic binder amounts and pressure schedules limiting spring-back, proved also quite helpful. Because most of the early technological research effort used the HPing approach, green body structure got less attention than it deserved. Most of the HP procedures focused – in the forming stage – only on ensuring good powder flow (for uniform die filling), giving less attention to the nano/micro scale of the green body. For instance granulation was done by spray drying. While generating granules which ensure good flow, this technique, if not perfectly tuned (the commercial spinel spray dried powders we examined do require much further improvement), leaves significant amounts of strong, porous aggregates in the green body thus significantly hampering densification. The real importance of the green-state, even when HP is used, is better understood now.[16] Consolidation by cold isostatic pressing, prior to hot pressing, is examined, especially for large parts.

In all cases where sintering to ≥97%TD under 1350 °C was achieved, the green body had an optimized structure.[10,23,69] The lowest AS temperature for attaining a sintered state density BD_A = 99%TD – made possible by the use of a special powder and the formation of an adequate green body – was reported to be in the 1150–1170 °C range.[69] Unfortunately no attempt to further densify, to transparency, was made by the authors.

2.2.1.3. Green body structure effect on densification: an example. In Fig. 5 the pores size distribution of powder compacts derived from three stoichiometric (X = 1.0) nano-powders (labeled SN1, SN2, SN3) is shown. As the figure shows, the green bodies differ both regarding the average size of the pores ($\bar{\phi}_P$) and the width of the distribution. A limitation of such graphs is the fact that they cannot tell which pores are of the intra-agglomerate and which of the inter-agglomerate variety. The influence on sintering pores of a given size exert, noticeably depends on their location. The size, morphology of the crystallites and the patterns of primary clusters configuration are illustrated in Fig. 6. Most of the crystallites are smaller than 70 nm (Figs. 6 and 7); the crystallites of SN3 are the finest. The

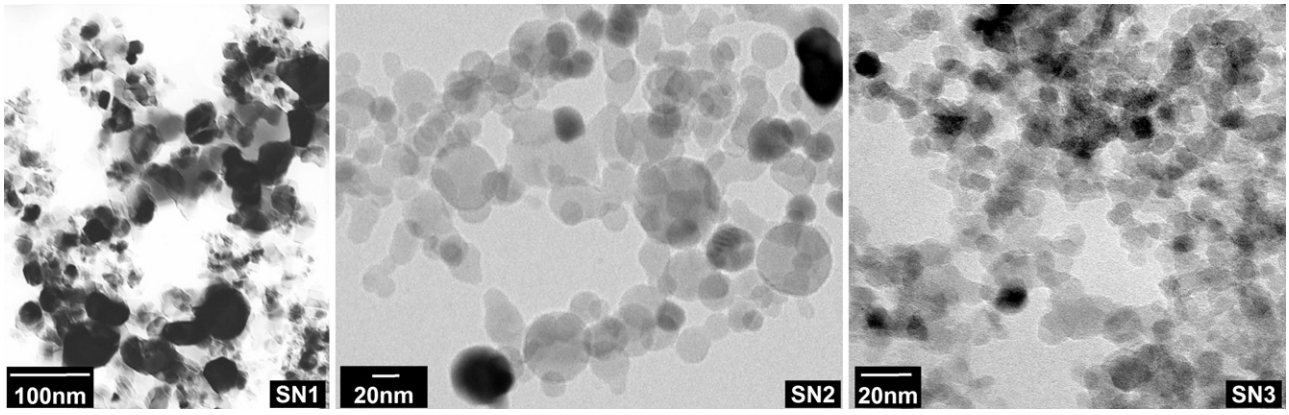

Fig. 6. Morphology, size and clustering pattern of powders SN1, SN2, SN3 crystallites (incipient sintering necks visible). TEM.

Please cite this article in press as: Goldstein A. Correlation between $MgAl_2O_4$-spinel structure, processing factors and functional properties of transparent parts (progress review). *J. Eur. Ceram. Soc.* (2012), doi:10.1016/j.jeurceramsoc.2012.02.051

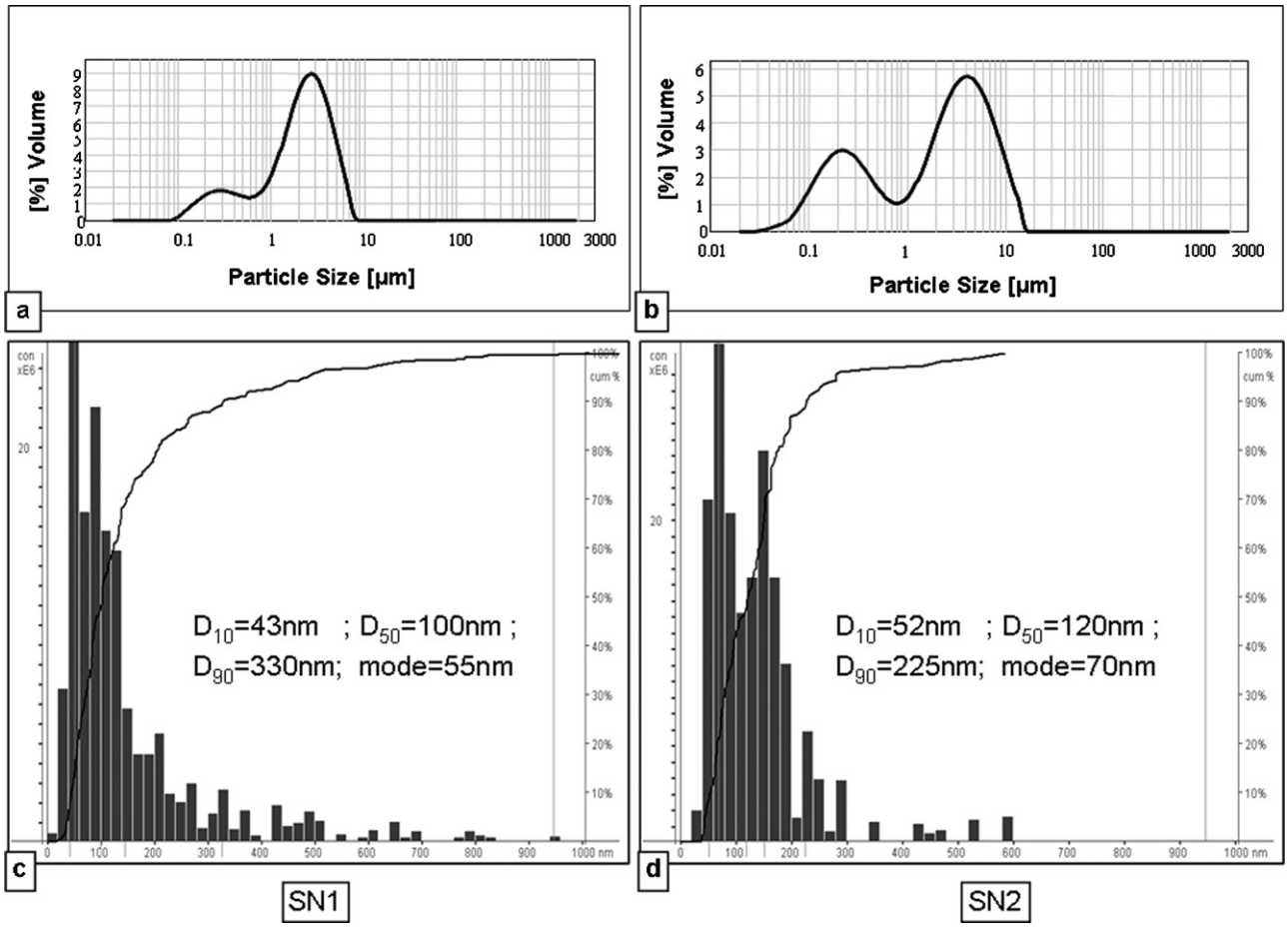

Fig. 8. Particles size distribution of spinel powders SN1, SN2 suspended in ethylene glycol (1.8% blown fish oil as deflocculant). Top: as received. Bottom: after agglomerates breaking (20 min attrition + low intensity ultrasonic field); D_{50} = median size of particles.

clustering pattern is specific to each powder. For the case of SN1, SN2 the size distribution in as-received and comminuted state are shown in Fig. 8. The SN3 initial material had a strong mode at ~6 μm and a fraction of particles under 1 μm much smaller than SN2; even after strong milling its median size was as high as ~3.5 μm.

In Fig. 9 the $BD_A = f$ sintering temperature ($T°_S$) curves are presented. As it can be seen, the $T°_S$ needed to cause advanced densification ($BD_A \geq 97\%TD$) significantly vary from material to material. The SN2 sinters satisfactorily at ~1300 °C, while the SN1 require a $T°_S$ of ~1500 °C; the SN3 is not dense enough even at 1700 °C.

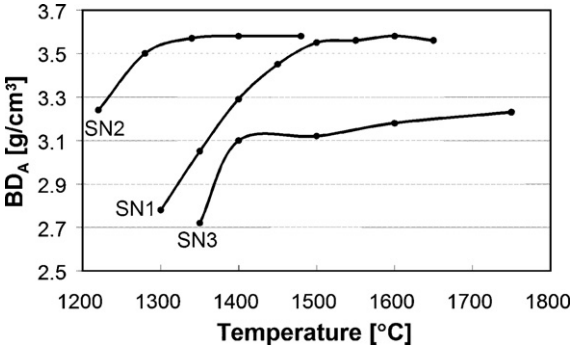

Fig. 9. Densification (AS) curves of green-bodies formed from powders SN1, SN2, SN3. SN1: $BD_g = 51\%TD$; SN2: $BD_g = 59\%TD$; SN3: $BD_g = 44\%TD$.

Besides green body structure, other factors can also influence sinterability.[77–85] The degree of influence of each factor is difficult to estimate in most cases. Here one of the important ones – the general disorder state of the powders' lattice – was estimated (only roughly). It was done by the aid of XRD data, following the method used in Ref. 69 (based on Ref. 28). The values obtained for the order degree (OD) parameter were: SN1 = 0.76, SN2 = 0.72, SN3 = 0.69. The OD values obtained are quite close and their order is different from that of sinterability. Therefore it is very likely that the observed differences in sinterability are caused mostly by variation in the green body structure, mainly pores size distribution, brought about by the different characteristics of the powders. Such a view seems to be substantiated by practice. In the case of the SN2 powder, densification[86] – of green bodies as they were at the start of the optimization process – required high temperatures, generating grains a few microns in size. Only after bringing the green body to the configuration shown in Fig. 5 was the sintering temperature reduced to 1300 °C.[23] Certain levels of correspondence exist between sinterability and a number of factors like powder particles size distribution (especially in the after milling state) or

Please cite this article in press as: Goldstein A. Correlation between $MgAl_2O_4$-spinel structure, processing factors and functional properties of transparent parts (progress review). *J. Eur. Ceram. Soc.* (2012), doi:10.1016/j.jeurceramsoc.2012.02.051

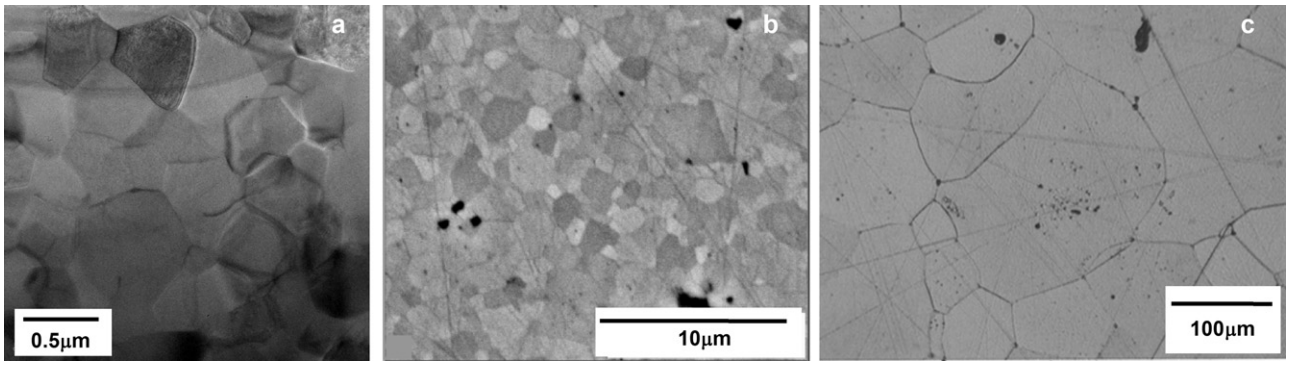

Fig. 10. Grains size distribution of densified spinels (SN1, SN2, and SN3) obtained at ICSI. (a)– SN2 after AS+HIP; $\overline{GS} = 0.5$ μm (ILT = 82%, $t = 2$ mm). (b) SN1 after AS + HIP; $\overline{GS} = 3.5$ μm (ILT = 79%, $t = 2$ mm). (c) SN3 after HP at 1780 °C; $\overline{GS} = 95$ μm; white, opaque.

ordering degree of the lattice. The highest level of direct correlation appears, however, between sintering temperature and green body pore size distributions.

In this example the main effect of the green body structure comes from the long "tail" of SN3 in the large size pores zone (Fig. 5). Such a green body (SN3) cannot be fully sintered even at $T°_S \geq 1700$ °C. The less pronounced, green structure, differences between SN1 and SN2 (Fig. 5) are still able to cause a change of ~200 °C in the temperature required to attain $BD_A = 97\%TD$. How important, especially for the mechanical properties (less for the optical), this difference is, can be seen in Fig. 10. While both SN2 and SN1 can be brought to a state of high transparency (ILT ≥ 80%) by HIPing, this happens at temperatures which keep the $\overline{GS}$ at ~0.5 μm for SN2, while raising the average grain size to ~3.5 μm for SN1. As a result the Vickers hardness ($\overline{HV5}$) is reduced from 14.5 to 13.8 GPa.

This comparison also allows one to put some numbers on the structural requirements for a sinterable green body. In order to attain a $BD_A = 97\%TD$, at a $T°_S \leq 1350$ °C, the n has to be <25 nm, the ratio between the maximal size (ϕ_M) and $\overline{\phi_P}$, $\phi_M/\phi_P < 1.5$, and $BD_g \geq 52\%TD$ (a correct $\overline{\phi_P}$ is of little help if the size distribution is not narrow enough).

2.2.1.4. Identification of the characteristics defining powder performance. The example above demonstrates how important the selection of a suitable raw material is (processing correction abilities are important, but limited) for the obtainment of sinterable green bodies. It shows that the differences in green body porosity characteristics – which control the maximal level of densification attainable – are, to a considerable extent, a result of differences in powder structure. SN2 is seen as an excellent raw material, SN1 – suitable, and SN3 – a disappointing one. Less clear is, however, why the SN2 powder is so performant. Which exactly are the characteristics which differentiate these powders, as to their ability to generate a suitable structure green body? Among the important features may be aspects currently not considered (some not easily measurable) when powder performance is estimated. Some of these features may affect the green body structure, others – the diffusion rate. Considering properties that might affect green structure, let us observe that the examined materials are roughly similar regarding some of the usually measured characteristics like crystallites and – for the case of SN1 and SN2 – as-milled particles size. The slight existing differences – regarding the size of basic particles – do not cause the effect expected, based on sintering theory formulated for compact arrangements of spherical non-agglomerated particles. Thus the SN3 powder is the finest powder ($d_{50} \sim 15$ nm) yet it generates a green body much less sinterable than those derived from the other two somewhat coarser powders.

Because, as shown above, the differences, regarding the usually measured properties, do not explain the behavior of the powders during pressing, it follows that influential differences exist concerning other aspects (rarely measured), like the strength of the aggregates (which controls behavior during comminution), their internal porosity, their surface chemistry (which influences inter-particle friction, during pressing) or morphology (which influences flow and arrangement pattern); the size and morphology of the agglomerates varies continuously during die filling and pressing. For instance, if surface interaction is strong, formation of large pores – by bonding, during pressing, of sets of particles (even very small ones) – is facilitated. The bonded particles define pores which they coordinate. In relation to such events it may be significant that the SN2 powder has spherical crystallites, while SN1 is based on faceted ones. As a result (and possibly also owing to differences in OH^- content on surface) the inter-particles friction is reduced in the case of the former, and more compact particles arrangement is made easier; hence the better green body structure (simultaneous finer pores and more compact particles arrangement). The powder behavior during compact forming is the resultant of the summation of these effects; coefficients quantifying the contribution of each effect need to be determined if one intends to make accurate prediction on green structure, based on measurements on powder.

Other powder characteristics, with influence on diffusion, like the type and level of disorder, also need attention, as shown by Krell et al.[37]

Establishment of an accurate and complete list of characteristics likely to influence powder sinterability, and estimation of their relative importance, is yet an only partially fulfilled task. Such a list, accompanied by measurements on the parameters of the list, would significantly reduce the amount of trial and

Please cite this article in press as: Goldstein A. Correlation between $MgAl_2O_4$-spinel structure, processing factors and functional properties of transparent parts (progress review). *J. Eur. Ceram. Soc.* (2012), doi:10.1016/j.jeurceramsoc.2012.02.051

error work needed in transparent spinel fabrication; it would allow powder sinterability level estimation through analysis of the data regarding the relevant characteristics.

2.2.2. *Microstructure in the final stage of sintering*

When full densification is the target, the green body structure is so important mostly because it has a strong influence, together with other features, on the microstructure during the last phase of the final stage of sintering (the one occurring when BD > 97%TD). The essential features of the structure, in that phase, are the amount, size distribution and location of the pores. In addition to green body structure, the characteristics of porosity, in the final stage of the sintering process, are determined by factors which exert their influence during firing, as shown below.

2.2.2.1. Influence of grain size. The most important microstructural feature is the grains size which, besides its influence, in all stages of sintering, on aspects like pores length and spacing (e.g. Ref. 4), controls an additional aspect, not carried by the kinetics equation, i.e. the fraction of the total porosity which is in an occluded state toward the end of the densification process. When final porosities <0.01% are sought, this fraction is critical, because such pores are much more difficult (sometimes impossible) to close than those attached to a grain boundary. The relationship between occlusion and GS is complicated also by the fact that once pore/grain boundary separation occurs (the "separation zone" defined in Ref. 77 is entered), the GS increase profile is changed owing to enhancement of abnormal grain growth. A suggestive example about the deleterious effect of occluded porosity is given by K. Tsukuma.[78] Of course coarsening enlarges also the "regular" pores, those in contact with the grain boundaries. Occluded porosity amount depends not only on $\overline{GS}$ but also on the GS distribution, because the critical density (ρ_C) over which the probability of occluded pores formation becomes significant is given[79] (case of pore drag control) by the relationship:

$$\rho_C = 1 - \left[\frac{\varepsilon}{3.3}\left(1 - \frac{\overline{GS}}{GS_M}\right)^3\right] \quad (6)$$

where ρ_C is the critical density; ε is the dielectric constant with a value dependent on the microstructural pattern.

Of course ΔGS is important also because if large it causes local variations of the densification rate (aspect not incorporated in (3) or similar) in real microstructures.

In Fig. 11 a schematic representation of the microstructure (at BD ≈ 97%TD) is given. The desired configuration "a" in which all residual pores are small and attached to grain boundaries may appear if the $\overline{GS}$ and ΔGS are small enough. For alumina[80,81] such a state [and consequent near full densification by pressureless sintering (PS)] was obtained for $\overline{GS}$~0.8 μm. In the case of Sp the maximal GS for which occlusion is negligible is not yet known. As Fig. 12 shows some occluded pores are present even at $\overline{GS}$ of ~1 μm; over 5 μm the fraction of occluded porosity noticeably increases and becomes massive for $\overline{GS}$ > 25 μm. This means that despite the fact that grain growth rate increase with temperature is moderate up to ~1650 °C (see

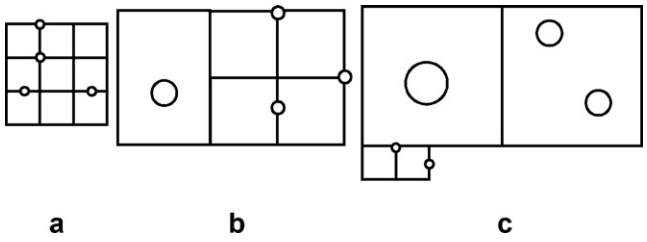

Fig. 11. Schematic representation of pores topology of spinel brought, by AS, to ~97%TD. (a) Ideal case; small pores attached to GBs of small grains. (b) Configuration allowing full densification state attainment; low fraction of occluded porosity. (c) Configuration precluding attainment of full densification state: large fraction of occluded porosity, large pores and grain size.

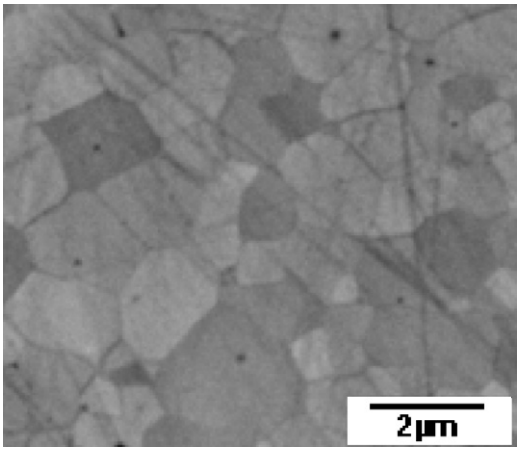

Fig. 12. Occluded porosity in fine grained ($\overline{GS}$ = ~1 μm) spinel after AS. SEM.

Fig. 13), and abnormal grain growth becomes marked only when $\overline{GS}$ exceeds ~20 μm, some occlusion has to be reckoned with when $T°_S$ > 1300 °C. Therefore in most practical cases the best microstructure achievable is better represented by situation "b" of Fig. 11; for $T°_S$ > 1650 °C situation "c" may also appear. The grain growth can also be limited by reducing the M_b. In the most difficult stage, when pore drag is lost, only solute or second phase drag may help (in the case of transparent spinel such a phase needs to exhibit $n \approx n_{Sp}$) in grain boundary mobility slowdown. These options are not well examined yet; they may, especially the first, prove as quite efficient. The grain growth may be influenced also by sintering aids. In transparent spinel

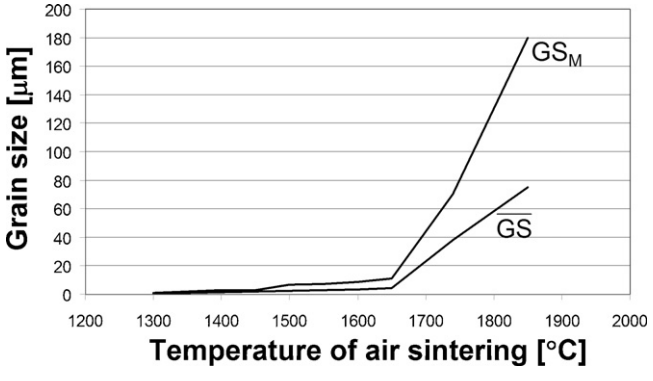

Fig. 13. Grains size ($\overline{GS}$, GS_M) as a function of AS temperatures (3 h dwell at peak temperature).

Please cite this article in press as: Goldstein A. Correlation between $MgAl_2O_4$-spinel structure, processing factors and functional properties of transparent parts (progress review). *J. Eur. Ceram. Soc.* (2012), doi:10.1016/j.jeurceramsoc.2012.02.051

fabrication, however, efficient sintering aids are difficult to come by owing to the requirement that they do not affect transmission. Besides the transient LiF, only B_2O_3 was reported as suitable.[78] The LiF, however, if not fully eliminated before closure, may generate many visible defects.[13,57] The oxide was demonstrated (0.15%[78] additive is optimal) as useful only for thin (~1 mm) disks ($T_{max} \sim 80\%$).

Besides its effect on densification, GS also influences mechanical properties. In order to obtain measurable values (e.g. HV5 > 13.5 GPa), the $\overline{GS}$ has to be lower than 3 μm; maximal values for the mechanical properties require a $\overline{GS}$~0.5 μm.[10,18,64]

Because the final stage microstructure is rarely ideal, it is essential to use another lever, indicated by Eq. (3): application of external pressure during sintering. The sintering stress for oxides[21,79] under PS conditions and considering 0.1–1 μm pores is lower than 20 MPa. Therefore adding external pressure (which may vary in the 40–200 MPa range, depending on procedure) significantly facilitates pores closure.

2.2.2.2. Influence of external pressure. Obtainment of transparent spinel by simple pressureless sintering, was of course, attempted from the start,[1,5,82] but neither high temperatures (>1800 °C), use of microwave fields[82–86] and/or high diffusivity atmospheres could raise the transmission over 50–60% (VIS). In most of these attempts, the general green structure was not well designed. However, even when this feature was somewhat improved and $T°_S$ reduction could be attained, the transparency achievable remained limited. In Fig. 3 (curve no. 3) the transmission spectrum of a disk – derived from a green body having a porosity like that shown in Fig. 6 (SN2), obtained by AS at 1380 °C/3 h – is shown. The ILT of only 50% (λ = 750 nm) is mostly a consequence of opaque spots (20 μm–2 mm) (see Fig. 14) generated by those regions in the green body where most of the residual pores are large ones, initially of the inter-agglomerate kind. The use of pressure is especially effective for the sintering of these loosely packed macro-agglomerate clusters; some such spots are always left after forming.

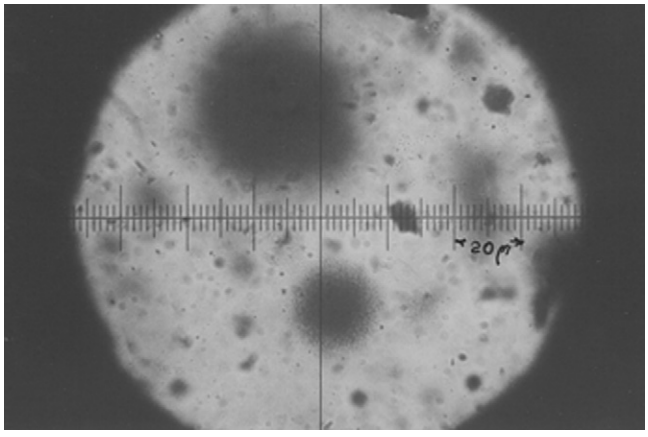

Fig. 14. Opaque, white spots in densified (AS) translucent, thin disk; spots generated by regions of unsuitable, green state, structure. Optical microscopy.

Pressure was used, from the early stages (D.W. Roy) of transparent spinel development, in the form of unidirectional hot pressing [including its more recent variant called – more or less correctly – spark plasma sintering (SPS)] and also as hot isostatic pressing (HIP).

The use of very high pressure (1–5 GPa range instead of the usual 30–50 MPa of regular HP and 60–120 MPa of SPS) allowed the obtainment of nano ($\overline{GS} = 50 - 60$ nm) grain size, because sintering was possible at temperatures lower than 1000 °C[20]; such specimens exhibit, though, only modest transmission values (~30%) as of now. The approach is difficult to upgrade to industrial scale. Special pressing schedules, based on gradual increase of pressure, also generated fine ($\overline{GS}$~1 μm) microstructure but associated with only moderate transparency.[12]

Another way to exploit the benefits of pressure is the use of a two steps sintering process in which the first stage brings the consolidated powder compact to 95–99%TD by PS (open porosity – OP ~ 0), and the second stage leads to a full densification state by the aid of HIPing. In such an approach the most important parameter is the HIPing temperature. At high temperatures diffusion rates are raised, but so is the grain growth rate; optimal tradeoffs need to be determined mostly by trial and error. It is also important to take, to HIPing, specimens exhibiting an optimal tradeoff between pores amount and GS. Practice showed that despite a higher pores content, ASed specimens having a BD_A of 96–97%TD attained, after HIPing, higher density than other with a BD_A of 99%TD.[64] The former had a lower $\overline{GS}$ and, probably more important, GS_M. The best ILT-GS-HV combinations yet reported were obtained using this approach.[16,23]

2.2.2.2.1. Reaction sintering. The use of pressure also alleviates, to some extent, the problems that may occur if the reaction preceded sintering approach[32,50,55] is used for Mg-spinel densification. In the case of Mg or Zn-spinels – as opposed to other double oxides like YAG – formation of the spinel from oxides engenders a significant volume variation, which may hamper densification.[87] This may explain the high temperatures needed for densification, and microcracking at grain boundaries (not observed in other sintering schemes), in approaches based on reaction preceded sintering, like those examined by A.F. Dercioglu et al.[50]

Regarding the reactive sintering approach it is worth noting, however, that despite the potentially deleterious effect mentioned in Ref. 87, in practice some interesting results were recently obtained by using it. For instance, M. Tanka et al.[88] and A. Ikesue et al.[89] have markedly improved the UV transmission of thick spinel parts by using partial or total reactive sintering (HP + HIP approach). Recently it was shown by A. Krell et al. that for a mixture corresponding to $X = 2.5$ an AS + HIP approach can generate, at temperatures usual in normal processing, plates ($t = 4$ mm) exhibiting a transmission spectrum (both ILT, TFT) identical to that of a single-crystal of the same composition.[37]

2.2.2.3. Comparison of pressure application techniques. The HP (usually under vacuum), while expensive, allows early application of pressure and processing of large parts; it can generate high quality transparent spinel. In fact, really large parts

Please cite this article in press as: Goldstein A. Correlation between $MgAl_2O_4$-spinel structure, processing factors and functional properties of transparent parts (progress review). *J. Eur. Ceram. Soc.* (2012), doi:10.1016/j.jeurceramsoc.2012.02.051

($L > 40$ cm) have been demonstrated, as of now, mostly by this method,[90–93] by companies like TA&T, NRL + MER or Surmet. A negative feature of most of the HP procedures reported is the generation of coarse microstructures (sometimes multimode GS distributions are observed) and strong discontinuous grain growth. The $\overline{GS}$ values are, usually, in the 40–90 μm range and, the largest grains fraction exhibit GS_M values in the 120–250 μm range; an example is shown in Fig. 10c. The main reason for this state of affairs was (and in some cases still is) the use of very high sintering temperatures. Accurate data on the temperatures used are relatively rare in the literature (mostly patents) describing HP procedures. However, comparing the data in Fig. 13 with Fig. 10c it becomes apparent that the latter imply temperatures ≥1750 °C. In our view such high temperatures are not a necessary feature of HPing. They are, to a considerable extent, the result of the less than optimal structure of the material in the green state. Recently progress was made by using cold isostatic pressing for the forming of green bodies; even for those of curved shape.[90,92] HP pressure levels are usually limited to ~70 MPa (by graphite strengths). The SPS variant seems to be able to offer more uniform, very fast heating, and, for low size specimens, high levels of pressure (60–110 MPa; even 200 MPa[55,94,95]). Large size parts, however, were not yet obtained. Carbon impurification is a problem in both techniques, being somewhat more severe in SPS machines (sputtering?). Up to now large transparent spinel parts made by HP come with large GS (GS > 20 μm). In the case of SPS, upgrading to large size, while feasible, seems very expensive.

In our view the HIPing (under pressures of 150–200 MPa of gas) of presintered Sp parts seems the most promising way to obtain reasonable cost parts for high performance. Finest microstructure spinel ($L \leq 25$ cm as of now) was obtained using this approach.[16,23] Large size and/or complex shape parts can be processed; suitable HIP machines are commercially available.

2.3. Macro scale (100 μm–1 m)

Selection of a suitable powder and application of adequate processing usually leads to the obtainment of green bodies exhibiting the desired structure in a large fraction of the part's volume. However, in most of the cases, a residual volume fraction – in which the pores size distribution is not conform with the requirements – is also present. It is made up of discrete regions which may have a size in the 50 μm–3 mm range (micro/macro defects). Such irregularities generated the white opaque "spots" (black in the transmission photo) shown in Fig. 14. Their size does not necessarily increase when that of the part is raised, but their volume density is usually larger. Some of these defects – which make obtainment, by PS, even of small transparent parts extremely difficult – may remain even after the high pressure sintering stage. Macro level flaws – like defective granules flow, non-uniform internal structure and strength not correlated with forming force – are among the causes of such defects. Getting rid of such defects, for large parts, is the most challenging task of those still confronting even the best technologies now available.

Warpage, especially of polygonal shaped plates (much less for disks), is also frequently seen; it originates, usually, from large scale fluctuation of the green density.

Delamination and cracks may result from the use of pressing schedules which do not match well powder characteristics.

Residual thermomechanical stress (which reduces noticeably mechanical strength) may also appear if cooling from $T°_S$ is too fast. Both warpage and stress start to become significant for a size >50 mm.

The grinding and polishing of the surfaces, while important and responsible for a large fraction of the fabrication costs, will not be treated in detail here. The major development of the last decade concerns polishing of curved surfaces by techniques like magnetorheological fluid finishing or chemical etching.

3. Performance, size and shape of transparent spinel parts obtainable by the developed techniques

In Table 1 the range of values, regarding the main parameters which decide transparent spinel performance, reported in the literature, is given. Values out of range (HV = 16–17.5 GPa, or TRS = 280–500 MPa) – which are either based on a single source and/or are not consistent with the structural data – are also reported in the literature; such values were not considered for Table 1. These values may prove correct (or be related to specific measurement conditions), but before accepting them further and independent confirmation is needed, together with plausible explanations based on structure-processing correlation.

The true performance level of transparent spinel parts can be estimated only considering the combination of the relevant properties, together with their size and shape. In Table 2 a few results, which constitute performance, are collected; the specific merit of each item is indicated. In Fig. 15 some transparent parts

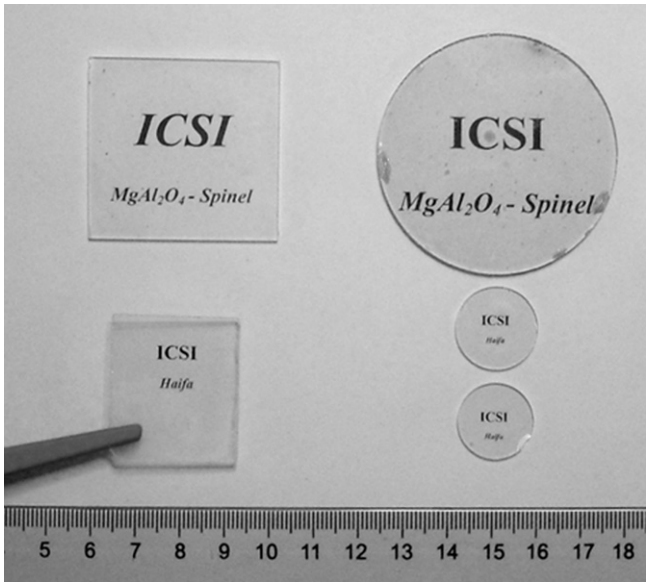

Fig. 15. Illustration of transparent spinel parts (ILT = 79–82%; λ = 800 nm; t = 2.0 mm) of various size and shape; left-bottom plate held at ~2 cm above background; fabricated at ICSI.

Please cite this article in press as: Goldstein A. Correlation between $MgAl_2O_4$-spinel structure, processing factors and functional properties of transparent parts (progress review). *J. Eur. Ceram. Soc.* (2012), doi:10.1016/j.jeurceramsoc.2012.02.051

(ICSI), of small to medium size, are shown. Their level of optical transmittance is shown in Fig. 1 (set of "colorless" curves).

4. Discussion: roadmap for further progress

Examination of the achievements and partially solved problems described above reveals certain ways of improving current practice, and allows identification of topics which need additional research. Thus it appears, first, that in order to attain the objectives listed in Section 1.2, a holistic research approach – in which the factors of influence, at all the scales, and their interaction, are considered – is needed. Not all effects are equal in strength, some of those operating at the nano/micro level being the most influential (Sections 2.2.1.3 and 2.2.2.1).

The evidence accumulated strongly suggests that the sintering strategy most able to generate acceptable cost products – in large quantities, exhibiting the required size and shape together with top performance – is a two stage process in which a pressureless initial firing (to 96–98%TD) is followed by a strong HIPing. It is clear now, however, that success of such an approach, especially for large parts, depends massively on the configuration of green body, much more so than in the case of hot pressing. The most important and difficult task (especially for large size and/or complex shape parts) is to form powder compacts in which the optimal nano/micro scales (see Section 2.2.1.3 last paragraph) structure is homogeneously maintained throughout the volume.

The extent to which the desired green structural pattern is achievable and can be kept constant throughout the volume depends critically on certain characteristics of the powder used. Neither the complete list of powder features relevant in this context, nor the true ranking of their importance, is fully understood. One of the main reasons for this is the poor understanding of the re-agglomeration process (during drying and pressing). Progress regarding this issue may bring substantial benefit. It was shown above, for instance, that the SN2 raw material allows the forming of highly sinterable green bodies. Currently the SN2 powder is prepared by a very expensive procedure (flame spray pyrolysis). Were it fully known what makes this material so performant, it is possible that less costly synthesis options could be found.

Insufficient attention devoted to the green state has kept, for a long time, the microstructure of hot pressed parts at a much coarser level than what it should have been (see Section 2.2.2.3).

It was also observed lately[64] that it is critical to ensure conditions for the limiting of occluded pores formation and elimination of those the apparition of which could not be prevented. In this context it was determined that the profile of the pressureless heating schedule and the way it is correlated with that of the HIPing stage are highly influential (e.g. Ref. 64).

The fact that the kind of optimization processes, suggested above for the green state and firing, may help, is supported by practice. The most efficient green body obtaining procedures were developed by the authors of 16. As a consequence they were the first to reduce the grain sizes of transparent spinel under 1 μm. Similar results were as of yet reported only by one other group[23] also as a consequence of green body structure improvement.

Manipulation of lattice structure for increasing of "good" diffusion rates is an additional (besides green structure improvement) powerful tool. Unfortunately understanding of phenomena occurring at this scale, especially point defects behavior, is vague yet.

5. Conclusions

The most difficult task, when high transparency spinel parts obtainment is the objective, is the reduction of the residual porosity under 100 ppm. If, in addition, the best possible mechanical properties are sought, the grains size needs to be kept under 1 μm. The residual porosity characteristics depend on the way the sintering process unfolds. The green body structure seems to be the strongest single factor of influence over sintering. The sintering is also influenced by other structural aspects, some of them interacting, like types and amount of point defects, lattice general order level and forms of disorder present, material stoichiometry, grain growth profile, impurities (especially carbon) present, sintering atmosphere composition and pores location. High transparency cannot be attained without pressure assistance during sintering. The most attractive approach for pressure application seems to be a two stage process in which AS (up to OP = 0) is followed by HIPing. Transparent spinel performance (for most of the important applications) can be quite well estimated considering a simple figure of merit which includes ILT and HV5-10. Specimens combining an ILT $\geq$ 82% with HV10 of up to 15 GPa (GS $\sim$ 0.5 μm) and L = 25 cm have been obtained. In other developments, large ($L \geq 30$ cm) plates and dome shaped parts of excellent transparency, but lower level mechanical properties, were fabricated.

References

1. Gatti A. Development of a process for producing transparent spinel bodies. Final Report. Contract N00019-69-C-0133, General Electric Co., Philadelphia Penn, 1969.
2. Roy DW. Hot pressed $MgAl_2O_4$ for UV–VIS and IR optical requirements. *Proc SPIE* 1981;**297**:13–8.
3. Cox JA, Greenlow D, Terry G, Fiedler L. Comparative study of advanced IR transmissive materials. *Proc SPIE* 1986;**683**:49–61.
4. Bergez P. Fabrication procedure of high performance $MgAl_2O_4$ parts especially parts transparent in VIS and IR. European Patent 0334760B1, May 1993.
5. Harris DC. History of development of polycrystalline optical spinel in the U.S. *Proc SPIE* 2005;**5786**:1–22.
6. Krell A, Hutzler T, Klimke J. Transparent ceramics for structural applications. Part 2: fields of applications. *Ber DKG* 2007;**84**:E50–5.
7. Strassburger E. Ballistic testing of transparent armor ceramics. *Proc ECerS X* 2007:2257–62.
8. Reimanis I, Kleebe HJ. A review on the sintering and microstructure development of transparent spinel ($MgAl_2O_4$). *J Am Ceram Soc* 2009;**92**:1472–80.
9. Krell A, Klimke J, Hutzler T. Transparent compact ceramics: inherent physical issues. *Opt Mater* 2009;**31**:532–6.
10. Krell A, Hutzler T, Klimke J. Advanced spinel and sub-μm Al_2O_3 for transparent armor applications. *J Eur Ceram Soc* 2009;**29**:275–81.
11. Apetz R, Van Bruggen MPB. Transparent alumina: a light scattering model. *J Am Ceram Soc* 2003;**86**:480–6.
12. Gazza GE, Dutta SK. Transparent ultrafine grained ceramics. US Patent 4,029,755; June 14 1977.

Please cite this article in press as: Goldstein A. Correlation between $MgAl_2O_4$-spinel structure, processing factors and functional properties of transparent parts (progress review). *J. Eur. Ceram. Soc.* (2012), doi:10.1016/j.jeurceramsoc.2012.02.051

13. Gilde G, Patel PJ, Patterson P, Blodgett D, Duncan D, Hahn D. Evaluation of hot pressing and hot isostatic pressing parameters on the optical properties of spinel. *J Am Ceram Soc* 2005;**88**:2747.
14. Reimanis IE, Kleebe HJ, Cook RL, DiGiovanni A. Transparent spinel fabrication from novel powders: synthesis, microstructure and optical properties. *Proc SPIE* 2004;**5429**:31–9.
15. Patel PJ, Gilde GA, Dehmer PG, McCawley JW. Transparent armor. *AMPTIAC Newsletter* 2000;**4**:1–13.
16. Krell A, Hutzler T, Klimke J. Transparent ceramics for structural applications. Part 1: physics of light transmission and technological consequences. *Ber DKG* 2007;**84**:E41–9.
17. Krell A, Hutzler T, Klimke J. Transmission physics and consequences for materials, selection, manufacturing and applications. *J Eur Ceram Soc* 2009;**29**:207–21.
18. Krell A, Hutzler T, Klimke J, Patthoff A. Nanoprocessing for larger fine grained windows of transparent spinel. *Cer Eng Sci Proc* 2010;**31**: 167–81.
19. Goldstein A, Chiriac V. *Spectroscopy of transition metal ions in vitreous matrices*. Timisoara: Timisoara Univ Press; 1988.
20. Lu TC, Chang XH, Qi JQ, Luo XJ, WEi QM, Zhu S, et al. Low temperature high pressure preparation of transparent nanocrystalline $MgAl_2O_4$ ceramics. *Appl Phys Lett* 2006;**88**:213120–3.
21. Lee SH, Kupp ER, Stevenson AJ, Anderson JM, Messing GL, Li X, et al. Hot isostatic pressing of transparent Nd:YAG ceramics. *J Am Ceram Soc* 2009;**92**:1456–63.
22. Helle AS, Easterling KE, Ashby ME. Hot isostatic pressing diagrams: new developments. *Acta Metall* 1985;**53**:2163–74.
23. Goldstein A, Goldenberg A, Hefetz M. Transparent polycrystalline $MgAl_2O_4$ spinel with submicron grains, by low temperature sintering. *J Ceram Soc Jap* 2009;**117**:1281–3.
24. Sickafus KE, Wills JM, Grimes NW. Spinel compounds: structure and property relations. *J Am Ceram Soc* 1999;**82**:5279–92.
25. Reddy KPR, Cooper AR. Oxygen diffusion in $MgAl_2O_4$ spinel. *J Am Ceram Soc* 1981;**64**:368–71.
26. Bacorisen D, Smith R, Uberuaga BP, Sickafus KE, Ball JA, Grimes RW. Atomistic simulations of radiation induced defect formation in spinels. *Phys Rev* 2006;**B74**, 214105-1–11.
27. Bordes N, Sickafus KE, Cooper EA, Ewing RC. Structural damage in spinel after ion irradiation. *J Nucl Mater* 1995;**225**:318–34.
28. Sickafus KE. Comment on: order–disorder phase transition induced by swift ions in $MgAl_2O_4$ and $ZnAl_2O_4$ spinels. *J Nucl Mater* 2003;**312**:111–23.
29. Jagodzinski H, Saalfeld H. Cation distribution and structural relations in Mg–Al spinel. *Z Kristallogr* 1958;**110**:197–218.
30. Uberuaga BP, Bacorisen D, Smith R, Ball JA, Grimes RW, Voter AF, et al. Defect kinetics in spinels: long-time simulations of $MgAl_2O_4$, $MgGa_2O_4$ and $MgIn_2O_4$. *Phys Rev* 2007;**B75**, 104116-1-13.
31. Ting CJ, Lu HY. Hot pressing of magnesium aluminate spinel. II – microstrcture development. *Acta Mater* 1999;**47**:831–40.
32. Ting CJ, Lu HY. Defect reactions and the controlling mechanism in the sintering of magnesium aluminate spinel. *J Am Ceram Soc* 1999;**82**:841–8.
33. Chiang YM, Kingery WD. Grain boundary migration in nanostoichiometric solid solutions of magnesium aluminate spinel: II. Effects of grain boundary nanostoichiometry. *J Am Ceram Soc* 1990;**73**:1153–8.
34. Ting CJ, Lu HY. Deterioration in the final stage sintering of magnesium aluminate spinel. *J Am Ceram Soc* 2000;**83**:1592–8.
35. Gritsyna VT, Afanasiev-Charkin IV, Kobyakov V, Sickafus KE. Structure and electronic states of defects in spinel of different compositions $MgO{\cdot}nAl_2O_3$:Me. *J Am Ceram Soc* 1999;**82**:3365–73.
36. Chiang YM, Kingery WD. Grain boundary migration in nanostoichiometric solid solutions of magnesium aluminate spinel: I. Grain growth studies. *J Am Ceram Soc* 1989;**72**:271–7.
37. Krell A, Waetzig K, Klimke J. Influence of the structure of $MgO{\cdot}nAl_2O_3$ spinel lattices on transparent ceramics processing and properties. *J Eur Ceram Soc*, this issue.
38. West GB, Perkins JM, Lewis MH. Characterization of fine grained oxide ceramics. *J Mater Sci* 2004;**39**:6687–704.
39. Aschauer U, Bowen P. Atomistic modeling study of surface segregation in Nd:YAG. *J Am Ceram Soc* 2006;**89**:3812–6.
40. Uberuaga BP, Smith R, Cleane AR, Montalenti F, Henkelman G, Grimes RW, et al. Structure and mobility of defects formed from collision cascades in MgO. *Phys Rev Lett* 2004;**92**:115505–8.
41. Gritsyna VT, Kazarinov YG, Moskvitin AO, Reimanis IE. Point defects in $MgAl_2O_4$ spinel doped with LiF. *Acta Phys Pol* 2010;**117**:161–5.
42. Belikh GI, Gritsyna VT, Udalova LV. Structure and mechanical properties of optical ceramics made of magnesium-alumina spinel. *Questions Atom Sci Tech* 2004;**85**:101–7.
43. Fang CM, Parker SC, de With G. Atomistic simulation of surface energy of spinel $MgAl_2O_4$. *J Am Ceram Soc* 2000;**83**:2082–4.
44. Hosseini SM. Structural, electronic and optical properties of spinel $MgAl_2O_4$. *Phys Stat Sol (b)* 2008;**245**:2800–7.
45. Ball JA, Pirzada M, Grimes RW, Zacate MO, Price DW, Uberuaga BP. Predicting lattice parameter as a function of cation disorder in $MgAl_2O_4$ spinel. *J Phys Condens Matter* 2005;**17**:7621–31.
46. Yong JS, Kang HN, Jiu Z, Yong L. Investigation on lattice constants of Mg–Al spinels. *J Mater Sci Lett* 2000;**19**:225–7.
47. Zawarah MF. Investigation of lattice constant, sintering and properties of nano Mg–Al spinels. *Mater Sci Eng* 2004;**A382**:362–70.
48. Zografou C, Reynen P, von Mallinckrodt D. Non-stoichiometry and sintering of MgO and $MgAl_2O_4$. *Interceram* 1983;**32**:40–3.
49. Shimada M, Endo T, Saito T, Sato T. Fabrication of transparent spinel polycrystalline materials. *Mater Lett* 1996;**28**:413–5.
50. Dercioglu AF, Boccaccini AR, Dlouhy I, Kagawa Y. Effect of chemical composition on the optical properties and fracture toughness of transparent magnesium aluminate spinel ceramics. *Mater Trans* 2005;**46**:996–1003.
51. Dillon SJ, Behera S, Harmer MP. An experimentally quantifiable solute drag factor. *Acta Mater* 2008;**56**:1374–9.
52. Powers JD, Glaeser AM. Grain boundary migration in ceramics. *Interface Sci* 1998;**6**:23–9.
53. Fan D, Chen SP, Chen LQ. Computer simulation of grain growth kinetic with solute drag. *J Mater Res* 1999;**14**:1117–20.
54. Rozenberg K, Reimanis IE, Kleebe HJ, Cook R. Chemical interaction between LiF and $MgAl_2O_4$ spinel during sintering. *J Am Ceram Soc* 2007;**90**:2038–42.
55. Meir S, Kalabukhov S, Frumin N, Dariel MP, Frage N. Synthesis and densification of transparent magnesium spinel by SPS processing. *J Am Ceram Soc* 2009;**92**:358–64.
56. Reimanis IE, Kleebe HJ. Reactions in the sintering of $MgAl_2O_4$ spinel doped with LiF. *Int J Mater Res* 2007;**98**:1273–8.
57. Villalobos G, Sanghera JS, Aggarwal ID. Degradation of magnesium aluminium spinel by LiF sintering aid. *J Am Ceram Soc* 2005;**88**:1321–2.
58. Woosley JD, Wood S, Jander E, Weeks R. Photoelectric effects in $MgAl_2O_4$ spinel. *Phys Rev* 1980;**22**:1065–7.
59. Mori K. Transient color centers caused by UV light irradiation in YAG crystals. *Phys Stat Sol* 1977;**A42**:375–8.
60. Bertrand-Granger G, Benameur N, Guizard C, Nygren M. Influence of graphite contamination on the optical properties of transparent spinel obtained by spark-plasma sintering. *Scripta Mater* 2009;**60**:164–7.
61. Kato H, Kodama T, Tamaura Y, Chang SG. Decomposition of CO_2 to carbon by hydrogen reduced Ni(II) bearing ferrite. *J Mater Sci* 1994;**29**: 5689–92.
62. Krasowska V, Winkler B, Yanowsky B. The color of sulphur. *J Phys Condens Matter* 1998;**10**:4093–100.
63. Krell A, Klimke J. Effects of the homogeneity of particle coordination on solid-state sintering of transparent alumina. *J Am Ceram Soc* 2006;**89**:1985–92.
64. Goldstein A, Goldenberg A, Vulfson M. Development of a technology for the obtainment of fine grain size, transparent $MgAl_2O_4$ spinel parts. *J Ceram Sci Technol* 2011;**2**:1–8.
65. Goldstein A, Ruginets R, Geffen Y. MW sintering of amorphous silica powders. *J Mater Sci Lett* 1997;**16**:310–2.
66. Lange FF. Sinterability of agglomerated powders. *J Am Ceram Soc* 1983;**67**:83–9.
67. Bratton RJ. Coprecipitation yielding $MgAl_2O_4$ spinel powders. *Am Ceram Soc Bull* 1969;**48**:759–62.
68. Mitchell P. Chemical method for preparing Mg-spinel. *J Am Ceram Soc* 1972;**55**:484–91.

Please cite this article in press as: Goldstein A. Correlation between $MgAl_2O_4$-spinel structure, processing factors and functional properties of transparent parts (progress review). *J. Eur. Ceram. Soc.* (2012), doi:10.1016/j.jeurceramsoc.2012.02.051

69. Behera SK. Synthesis of Mg–Al spinel from autoignition of citrate-nitrate gel. *Matto Lett* 2004;**58**:1451–4.
70. Al-Sharab J, Cosandey F, Singhal A, Skandan G. TEM characterization of nano structured $MgAl_2O_4$. Synthesis by direct conversion synthesis for γAl_2O_3. *J Am Ceram Soc* 2006;**89**:2279–85.
71. Lange FF. Powder processing science and technology for increased reliability. *J Am Ceram Soc* 1989;**72**:3–15.
72. To D, Rajesh D, Yin X, Sundareson S. Deagglomeration of nanoparticle aggregates via rapid expansion of supercritical or high pressure suspensions. *Am Ind Chem Eng J* 2009;**55**:2807–26.
73. Kitayama M, Pask JA. Formation and control of agglomerates in alumina powders. *J Am Ceram Soc* 1996;**79**:2003–11.
74. Rawle A. Nanoceramics – stepping back to the future. *Am Ceram Soc Bull* 2009;**86**:37–9.
75. Neisz DE, Benett RB, Snyder MJ. Strength characterization of powder aggregates. *Bull Am Ceram Soc* 1972;**51**:677–80.
76. Horn RG. Surface forces and their action in ceramic materials. *J Am Ceram Soc* 1990;**73**:1117–35.
77. Brook RJ. Pore-grain boundary interactions and grain growth. *J Am Ceram Soc* 1969;**52**:56–7.
78. Tsukuma K. Transparent $MgAl_2O_4$ spinel ceramics produced by HIP post sintering. *J Ceram Soc Jap* 2006;**114**:802–6.
79. German RM. *Sintering theory and practice*. New York: J. Wiley; 1996.
80. Coble RL. Sintering crystalline solids. II – Experimental test o diffusion models in powder compacts. *J Appl Phys* 1961;**32**:792–9.
81. Kang SJ, Jung YL. Sintering kinetics at final stage sintering. *Acta Mater* 2004;**52**:4073–8.
82. Bratton RJ. Translucent sintered $MgAl_2O_4$. *J Am Ceram Soc* 1974;**57**:283–6.
83. Cheng J, Agrawal D, Zhang Y, Drawl B, Roy R. Fabricating transparent ceramics by MW sintering. *Bull Am Ceram Soc* 2000;**79**:71–4.
84. Gilde G, Patel P, Patterson M. A comparison of hot-pressing, rate controlled sintering and microwave sintering of magnesium aluminate spinel for optical applications. *Proc SPIE* 1999;**3705**:94–104.
85. Goldstein A, Geifman L, Bar-Ziv S. Susceptor assisted microwave sintering of $MgAl_2O_4$ powder at 2.45 GHz. *J Mater Sci Lett* 1998;**17**:977–9.
86. Goldstein A, Goldenberg A, Yeshurun Y, Hefetz M. Transparent $MgAl_2O_4$ spinel from a powder prepared by flame spray hydrolysis. *J Am Ceram Soc* 2008;**91**:4141–4.
87. Hong WS, DeJonghe LC, Yang X, Rahaman MN. Reaction sintering of $ZnO–Al_2O_3$. *J Am Ceram Soc* 1995;**78**:3217–24.
88. Tanaka M, Takahasi T, Hatomoto S. Spinel sintered material. Int Patent Application WO 2009/128269A1, 16.04.2009.
89. Ikesue A. Transparent spinel ceramic, method for production thereof, and optical material using the transparent ceramic. Int Patent Application WO 2008/090909A1, 23.01.2008.
90. Aggarwal I, Bayya S, Villalobos G, Kim W, Sanghera J. Recent developments in transparent polycrystalline spinel for electro-optical applications. *SPIE Proc* 2009;**7302**, 7302F-1–8.
91. Tsai DS, Wang CT, Yang SJ, Hsu SE. Hot isostatic pressing of $MgAl_2O_4$ spinel windows. *Mater Manuf Proc* 1994;**9**:709–10.
92. La Roche A, Kutsch J, Rozenberg K, Fehrenbacher L. Manufactring issues for polycrystalline transparent spinel domes. *SPIE Proc* 2009;**7302**, 7302D-1–8.
93. Ting CJ, Lu HY. Hot pressing of magnesium aluminate spinel. I – kinetics and densification mechanisms. *Acta Mater* 1995;**47**:817–30.
94. Morita K, Kim BN, Hiraga K, Yoshida H. Fabrication of high strength transparent $MgAl_2O_4$ spinel polycrystals by optimizing spark plasma sintering conditions. *J Mater Res* 2009;**24**:2863–72.
95. Frage N, Cohen S, Meir S, Kalabukhov S, Dariel MP. Spark plasma sintering (SPS) of transparent magnesium-aluminate spinel. *J Mater Sci* 2007;**42**:3273–5.

Please cite this article in press as: Goldstein A. Correlation between $MgAl_2O_4$-spinel structure, processing factors and functional properties of transparent parts (progress review). *J. Eur. Ceram. Soc.* (2012), doi:10.1016/j.jeurceramsoc.2012.02.051